Hierarchical Self-Assembly, Coassembly, and Self-Organization of Novel Liquid Crystalline Lattices and Superlattices from a Twin-Tapered Dendritic Benzamide and Its Four-Cylinder-Bundle Supramolecular Polymer

Virgil Percec,*[a, c] Tushar K. Bera,[a] Martin Glodde,[a, c] Qiongying Fu,[a] Venkatachalapathy S. K. Balagurusamy,[a, b, c] and Paul A. Heiney[b, c]

Abstract: The synthesis and structural analysis of the twin-dendritic benzamide **10**, based on the first-generation, self-assembling, tapered dendrons 3,4,5-tris(4′-dodecyloxybenzyloxy)benzoic acid and 3,4,5-tris(4′-dodecyloxybenzyloxy)-1-aminobenzene, and the polymethacrylate, **20**, which contains **10** as side groups, are presented. Benzamide **10** self-assembles into a supramolecular cylindrical dendrimer that self-organizes into a columnar hexagonal (Φ_h) liquid crystalline (LC) phase. Polymer **20** self-assembles into an imperfect four-cylinder-bundle supramolecular dendrimer, and creates a giant vesicular supercylinder that self-organizes into a columnar nematic (N_c) LC phase which displays short-range hexagonal order. In mixtures of **20** and **10**, **10** acts as a guest and **20** as a host to create a perfect four-cylinder-bundle host–guest supramolecular dendrimer that coorganizes with **10**. A diversity of Φ_h, simple rectangular columnar ($\Phi_{r\text{-}s}$) and centered rectangular columnar ($\Phi_{r\text{-}c}$), superlattices are produced at different ratios between **20** and **10**. This diversity of LC lattices and superlattices is facilitated by the architecture of the twin-dendritic building block, polymethacrylate, the host–guest supramolecular assembly, and by hydrogen bonding along the center of the supramolecular cylinders generated from **10** and **20**.

Keywords: dendrimers · four-cylinder-bundle · liquid crystals · self-assembly · superlattices ·

Introduction

Dendrimers, dendrons, and more complex dendritic building blocks provided some of the most influential architectural motifs and have had a remarkable impact on the field of science at the interface between chemistry, biology, physics, and complex ordered soft-condensed matter.[1–3] Our laboratory is involved in the elaboration of synthetic strategies for the preparation of self-assembling dendrons, more complex functional self-assembling dendritic building blocks,[4] and of macromolecules based on them.[5] The supramolecular dendrimers and dendritic macromolecules, generated from the self-assembly of these molecular and macromolecular dendritic building blocks, have the shape perfection to allow self-organization into a large variety of 2D and 3D liquid-crystalline[4c] lattices, such as: *p6mm* hexagonal columnar,[4a,e,g,n] *c2mm* rectangular columnar,[4p] various smectic phases,[4q, 6] $Pm\bar{3}n$ cubic,[4f,n] $Im\bar{3}n$ cubic,[4n, 5j, k] cybotactic nematic phases,[6] and others. The research on the discovery of new LC lattices from self-assembling dendritic building blocks continues, both in our, and in other laboratories.[7]

Previously, we have reported on a novel architectural concept and a strategy derived from it, which we believe will provide a universal approach to the design of a diversity of new LC superlattices.[4i] This concept is based on twin-dendritic benzamides and polymers containing twin-dendritic benzamide side groups. Previously,[4i] we have shown that the simplest twin-dendritic benzamide based on the AB_3 mini-dendritic building block,(3,4,5-tris(*n*-alkan-1-yloxy)benzoic acid and 3,4,5-tris(*n*-alkan-1-yloxy)-1-aminobenzene),[4n] self-assembles into supramolecular cylindrical dendrimers that self-organize into a 2D hexagonal columnar (Φ_h) LC phase. The corresponding polymethacrylate containing the same twin-dendritic side-groups self-assembles into a three-

[a] Prof. V. Percec, Dr. T. K. Bera, Dr. M. Glodde, Q. Fu, Dr. V. S. K. Balagurusamy
Roy & Diana Vagelos Laboratories
Department of Chemistry, University of Pennsylvania
Philadelphia, 19104-6323 (USA)
Fax: (+1) 215-573-7888
E-mail: percec@sas.upenn.edu

[b] Dr. V. S. K. Balagurusamy, Prof. P. A. Heiney
Department of Physics and Astronomy
University of Pennsylvania
Philadelphia, 19104-6323 (USA)

[c] Prof. V. Percec, Dr. M. Glodde, Dr. V. S. K. Balagurusamy, Prof. P. A. Heiney
Laboratory for Research on the Structure of Matter
University of Pennsylvania
Philadelphia, 19104-6323 (USA)

  0947-6539/03/0904-0921 $ 20.00+.50/0

cylinder-bundle supramolecular dendrimer, which self-organizes into a nematic phase. The co-assembly of the 20 and 60 mol % of twin-dendritic benzamide, with up to 80 mol % of the three-cylinder-bundle supramolecular dendrimer, produced a novel hexagonal columnar LC superlattice.[4i]Hydrogen bonding along the center of the supramolecular column is an important structural parameter that determines the self-assembly and coassembly of these twin-dentritic building blocks. This result was rewarding, since it demonstrated the potential use of this new and simple concept for the elaboration of other novel LC superlattices from twin-dendritic building blocks. In our laboratory we have access to a library of self-assembling dendrons; [4n] therefore, strategies derived from symmetric twin-, and asymmetric di-dendritic building blocks, based on this library, could provide easy access to novel dendritic architectural motifs, without using the synthetic effort involved in the design and preparation of novel self-assembling dendrons.

This present publication is the second on this topic and addresses the generality and universality of this concept. Therefore, in the series of experiments reported here we have employed the second most frequently studied, AB_3 first generation self-assembling dendrons (3,4,5-tris(4′-dodecyloxybenzyloxy)benzoic acid and 3,4,5-tris(4′-dodecyloxybenzyloxy)-1-aminobenzene) in our laboratory[4a,e,g,n] to synthesize the corresponding twin-dendritic benzamide and polymethacrylate, containing the twin-dendritic benzamide as side groups. As expected, the new twin-dendritic benzamide reported here self-assembles into a supramolecular cylindrical dendrimer, which self-organizes into a Φ_h LC lattice by similar principles to those previously reported. [4i] Its corresponding polymer self-assembles into an imperfect four, rather than a three-cylinder-bundle supramolecular dendrimer, as the previous system did.[4i] The imperfect four-cylinder-bundle supramolecular dendrimer resembles a vesicular supercylinder that self-organizes into a columnar nematic (N_c) phase and displays short-range hexagonal order. Co-assembly of the twin-dendritic benzamide with its corresponding polymer provides, depending on the molar ratio between the two components, a Φ_h superlattice, a simple-rectangular columnar superlattice ($\Phi_{r\text{-}s}$), a centered-rectangular columnar superlattice ($\Phi_{r\text{-}c}$), and a Φ_h lattice. During these co-assembly processes, the four-cylinder-bundle supramolecular dendrimer undergoes structural changes from a vesicular supercylinder, generated from an imperfect to a perfect four-cylinder bundle supramolecular dendrimer. The transition from an imperfect four to a perfect four-cylinder-bundle supramolecular dendrimer is facilitated by the host–guest interactions between the empty spaces of the imperfect four-cylinder bundle, which acts as a host, and the twin-dendritic benzamide, which acts as a guest. The diversity of novel architectural motifs and superlattices reported here demonstrates that the twin-dendritic benzamide concept has great potential to contribute to the enrichment of functional complex and ordered soft condensed matter, derived from self-assembling dendritic building blocks.[8]

Results and Discussion

Synthesis of twin-dendritic benzamide 10 and twin-dendritic benzamide monomer 19: Schemes 1 and 2 show the synthesis of the twin-dendritic benzamide *N*-[3,4,5-tris(4′-dodecyloxybenzyloxy)phenyl]-3,4,5-tris(4′-dodecyloxybenzyloxy) benz-

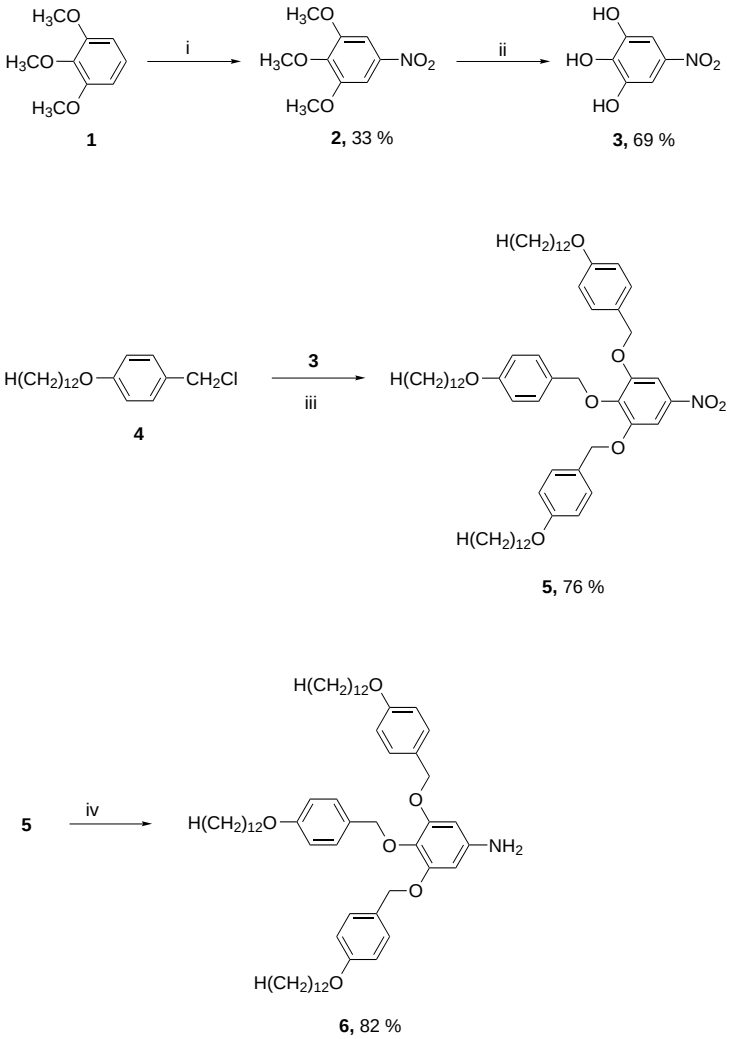

Scheme 1. i) CH_2Cl_2, $SiO_2 \cdot HNO_3$, 20 °C; ii) Py · HCl, 200 °C, 1 h; iii) K_2CO_3, DMF, 70 °C ; iv) $NH_2NH_2 \cdot H_2O$, graphite, EtOH, reflux.

0947-6539/03/0904-0922 $ 20.00+.50/0 *Chem. Eur. J.* **2003**, *9*, No. 4

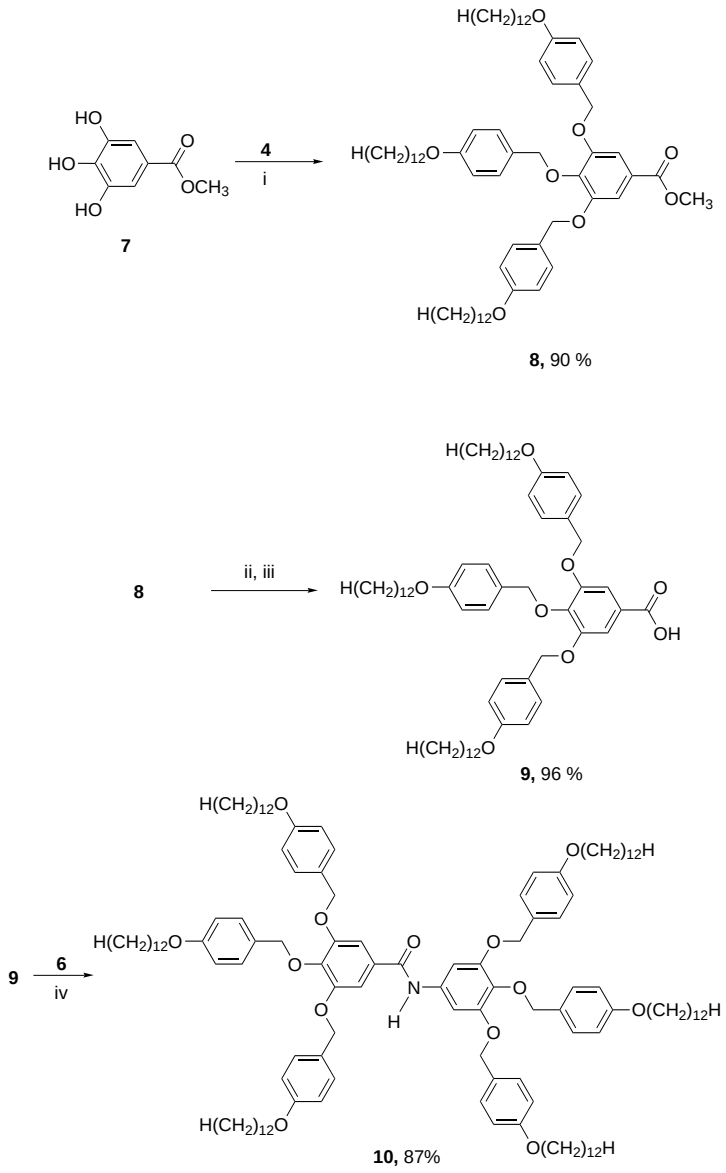

Scheme 2. i) K_2CO_3, DMF, 70 °C; ii) KOH/H_2O, EtOH; iii) HCl, THF; iv) DCC, DPTS, CH_2Cl_2.

amide (**10**). 1,2,3-Trimethoxybenzene (**1**) was nitrated with HNO_3 supported on SiO_2[4i, 8–11] at 20 °C for 15 minutes to produce 3,4,5-trimethoxy-1-nitrobenzene (**2**) in 33 % yield. This nitration procedure eliminates the oxidative demethylation and selectively places the nitro group at the 5-position of **1**.[4i, 10, 11] Demethylation of **2** with Py · HCl salt in melt state (200 °C) for 1 h produced 3,4,5-trihydroxy-(1-nitrobenzene) (**3**) in 69 % yield. Compound **3** was alkylated with 4-dodecyloxy(benzyl chloride) (**4**) by using anhydrous K_2CO_3 as a base in DMF at 70 °C to produce 3,4,5-tris(4′-dodecanoxybenzyloxy)-1-nitrobenzene (**5**) in 76 % yield. Reduction of **5** with $NH_2NH_2 \cdot H_2O$ over graphite powder[4i, 10–12] in ethanol generated 3,4,5-tris(4′-dodecyloxybenzyloxy)-1-aminobenzene (**6**) (82 % yield).

3,4,5-Tris(4′-dodecyloxybenzyloxy) benzoic acid (**9**) was synthesized by the alkylation of methyl-3,4,5-trihydroxybenzoate (methyl gallate) (**7**) with **4**, followed by the hydrolysis of the resulting compound **8** with KOH in EtOH at reflux (96 % yield; Scheme 2).[4a] Amidation of **9** with **6** was carried out under neutral conditions (DCC/DPTS)[5d] to produce **10** in 87 % yield.

The synthesis of monomethacrylate functionalized twin-dendritic benzamide monomer **19** is outlined in Scheme 3 and 4. The first step requires the protection of two phenol groups from the 4- and 5-positions of methyl gallate (**7**) (Scheme 3). The cleavage of the protecting group had to be performed under neutral conditions, since the benzyl ether group of **13** does not tolerate acidic conditions. A benzo[1,3]-dioxole group was employed for this purpose.[13] This protecting group was cleaved under neutral conditions without affecting the integrity of the benzyl ether group from **13**. Thus, 2-ethoxy-7-hydroxybenzo[1,3]-dioxole-5-carboxylic acid methyl ester (**11**) was synthesized in 57 % yield by condensing ethyl *ortho*-ester with **7** in the presence of Amberlyst-120 resin as a catalyst at 130 °C for 18 h. The hydroxy group of **11** was subsequently etherified with 4-(11-hydroxyundecyloxy)benzyl chloride (**12**) in DMF at 70 °C, by using K_2CO_3 as a base to yield 2-ethoxy-7-[4′-(11′-hydroxyundecyloxy)benzyloxy]-benzo[1,3]-dioxole-5-carboxylic acid methyl ester (**13**) in 72 % yield. The dioxole protecting group was cleaved in SiO_2 by refluxing MeOH to produce 3,4-dihydroxy-5-[4′-(11′-hydroxyundecanoxy)benzyloxy]methyl benzoate (**14**) in 91 % yield. In the subsequent step (Scheme 3), the alkylation of **4** with **14**, using similar conditions (K_2CO_3/DMF) to those employed in the synthesis of **5**, yielded 3,4-bis(4′-dodecyloxybenzyloxy)-5-[4′-(11′-hydroxyundecyloxy)benzyloxy]methyl benzoate (**15**) in 79 % yield. The basic hydrolysis of **15** with aqueous KOH in refluxing MeOH yielded the corresponding benzoic acid **16** in 91 % yield. Compound **16** was esterified with methacryloyl chloride using Et_3N in CH_2Cl_2 at 0–5 °C to produce the methacrylate-functionalized twin-dendritic monomer 3,4-bis(4′-dodecyloxybenzyloxy)-5-[4′-(11′-methacryloxyundecyloxy)benzyloxy]benzoic acid (**18**). The intermediate, mixed benzoic methacryloyl anhydride (**17**), was hydrolyzed with Py/H_2O at 130 °C (Scheme 4). Amidation of **18** with **6** was carried out in THF at 20 °C by using DCC/DPTS[5d] to produce the monomethacrylate functionalized twin-dendritic benzamide

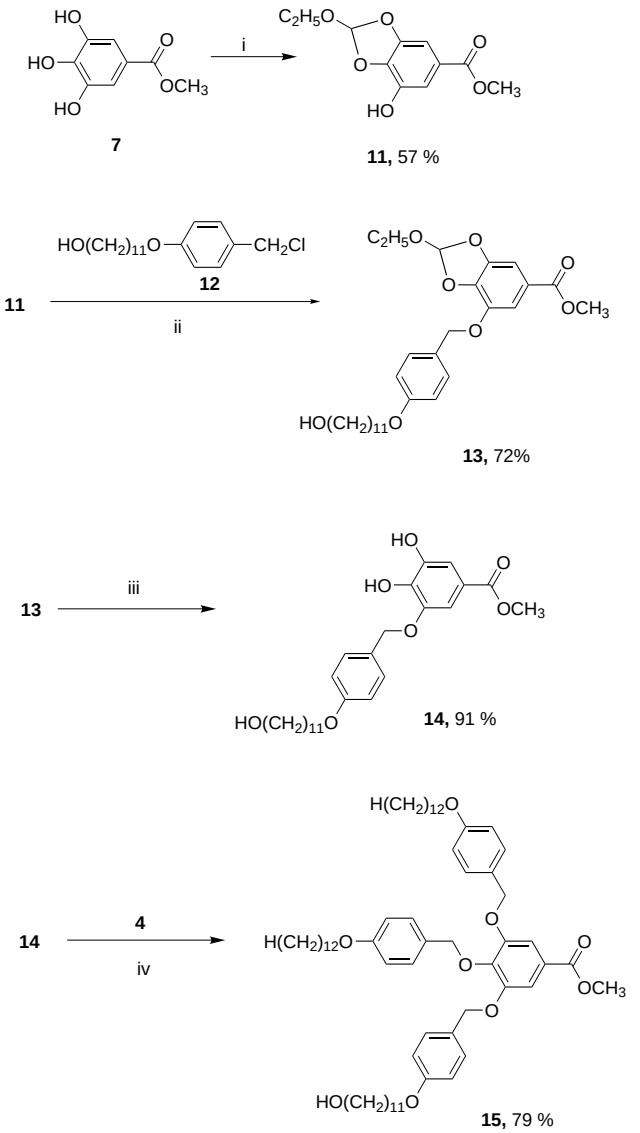

Scheme 3. i) $(EtO)_3CH$, Amberlyst-120, 130 °C, 18 h; ii) K_2CO_3, DMF, 70 °C; iii) SiO_2, MeOH, reflux, 24 h; iv) K_2CO_3, DMF, 70 °C.

N-[3,4,5-tris(4′-dodecanoxybenzyloxy)phenyl]-3,4-bis(4′-dodecanoxybenzyloxy)-5-[4′-(11′-methacryloxyundecanoxy) benzyloxy]benzamide (**19**), in 70% yield after purification by column chromatography (SiO_2, hexanes/EtOAc 9:1).

Polymerization of 19: Radical polymerization of **19** initiated by AIBN was carried out under N_2 in benzene at 60 °C (Scheme 5) for 18 h to achieve a high conversion (93%). The resulting polymer was purified by column chromatography (Al_2O_3, hexanes) to separate the unreacted monomer. $M_n =$ 49.813 and $M_w/M_n = 1.62$ (GPC with polystyrene standards).

Thermal analysis of 10, **19**, **and 20**: All compounds were analyzed by a combination of differential scanning calorimetry (DSC), thermal optical polarized microscopy (TOPM), and X-ray diffraction (XRD) experiments. The transition temperatures and the corresponding enthalpy changes (kcal mol^{-1}) were determined by DSC with a heating/cooling rate of 10 °C min^{-1}. The assignment of various phases was done by a combination of XRD and TOPM according to standard methods employed in our laboratory.[4i,n]

Table 1 summarizes the transition temperatures and the corresponding enthalpy changes for **10**, **19**, and **20**. Both twin-dendritic benzamides **10** and **19** exhibit an enantiotropic hexagonal columnar (Φ_h) liquid crystalline (LC) phase. In both cases, the Φ_h phase was confirmed by XRD. The degree of supercooling of $T_{i\text{-}\Phi h}$ is, as expected, low: 9 °C for **10** and 7.5 °C for **19**. Introduction of a methacryloyl group on the periphery of **10** decreases the thermal stability of the mesophase and reduces the isotropization temperature of **19** by 14 °C. This destabilization is due to the unsymmetric substitution of **19** (Table 1).

During heating, polymer **20** exhibits an LC phase that undergoes isotropization at 163 °C. A columnar nematic (N_c) LC phase was assigned by a combination of TOPM and XRD studies for this phase. A detailed discussion of the XRD analysis will be presented later. Due to the slow dynamics of polymer **20**, the isotropization peak is not seen during the second heating and cooling DSC scans. However, on all heating and cooling scans, the isotropization temperature was detected by TOPM and XRD experiments.

Structural analysis of 10, **19**, **and 20**: Powder samples of **10**, **19**, and **20** were studied both at room temperature, and in the temperature range over which they form the LC phase. In the work described here, we use the convention $q = (4\pi/\lambda) \cdot \sin(\theta) = 2\pi/d$, in which 2θ is the scattering angle and d is the interplanar spacing. Due to the appearance of weaker peaks on top of the diffuse scattering, and the background scattering, the peak positions were determined after curve fitting all the diffraction patterns. Figure 1 shows the powder diffraction patterns of **10**, **19**, and **20**.

Structural analysis of twin-dendritic benzamide 10: The twin-tapered dendritic molecule **10** exhibits one strong and one weak, but sharp, diffraction peak in the LC phase (**20**/**10** (0:100) in Figure 1; Table 2). The calculated ratio of the interplanar spacing of the strong peak to that of the weak peak is $d_{10}/d_{11} = 1.70$ ($\approx \sqrt{3}$). Thus, these peaks arise from the Φ_h lattice formed by the twin-dendritic supramolecular cylinder self-assembled from **10** and were indexed as (10) and (11). The (10) peak is superimposed on a relatively weak diffuse maximum at approximately the same peak position. This diffuse scattering cannot arise from any static structural disorder, since it does not show any noticeable change upon annealing at high temperature. Most probably, it arises from column undulations like that observed in the Φ_h phases obtained from discotic molecules, such as alkoxy-substituted triphenylene.[14] The (11) peak does not show any detectable diffuse scattering underneath. Additionally, a very broad diffuse peak in the wide angle was observed; this corresponds to the liquidlike short-range order of the melted alkyl tails.

The simplified molecular model of **10** containing only methoxy tails, generated with the aid of the Macro Model version 6.5 software (Columbia University) on a Silicon Graphics O_2, is shown in Figure 2 (middle section). The twin-dendritic benzamide **10** produces a criss-crossed stack as illustrated in the top view of the model (Figure 2, mid right).

0947-6539/03/0904-0924 $ 20.00+.50/0 *Chem. Eur. J.* **2003**, *9*, No. 4

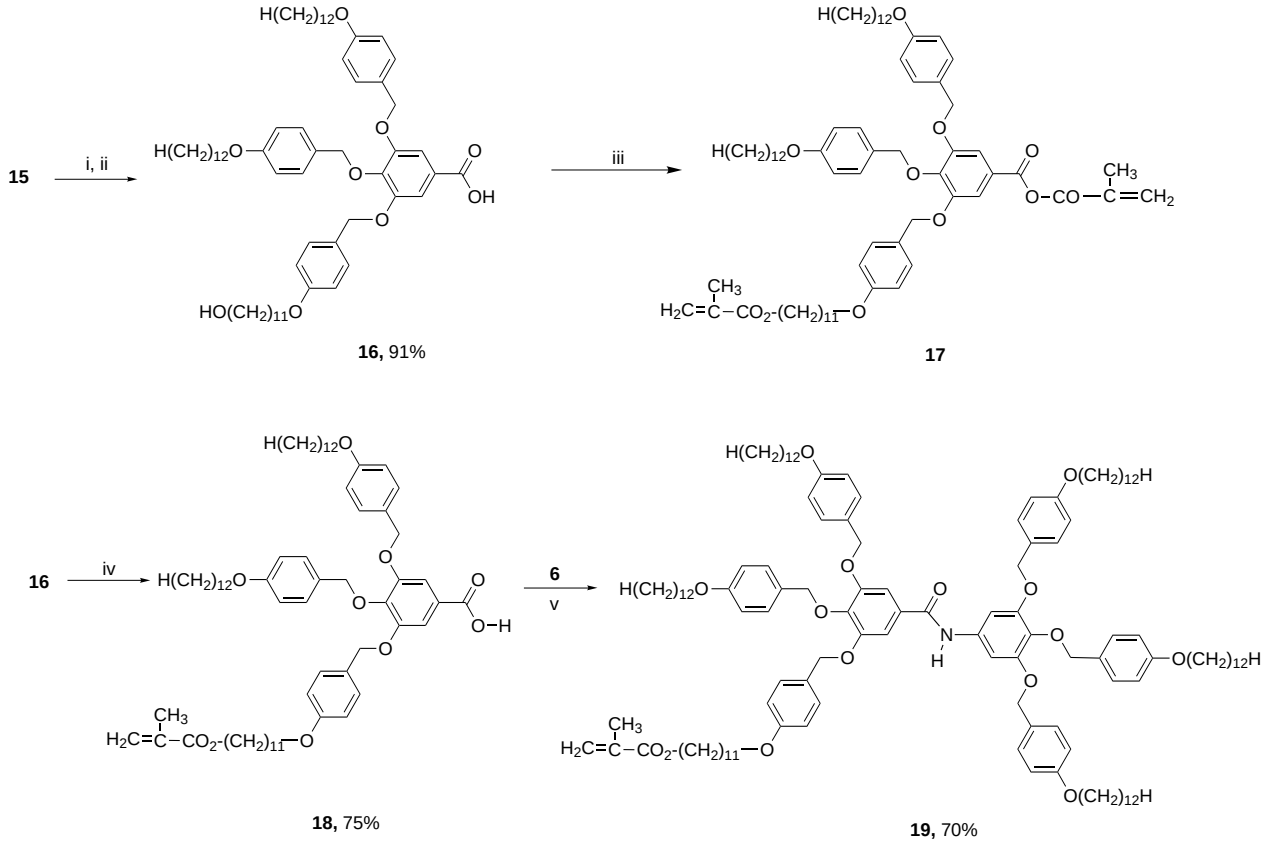

Scheme 4. i) KOH/H_2O, EtOH; ii) HCl, THF; iii) methacryloyl chloride, CH_2Cl_2, Et_3N; iv) pyridine/H_2O, 130 °C; v) DCC, DPTS, THF.

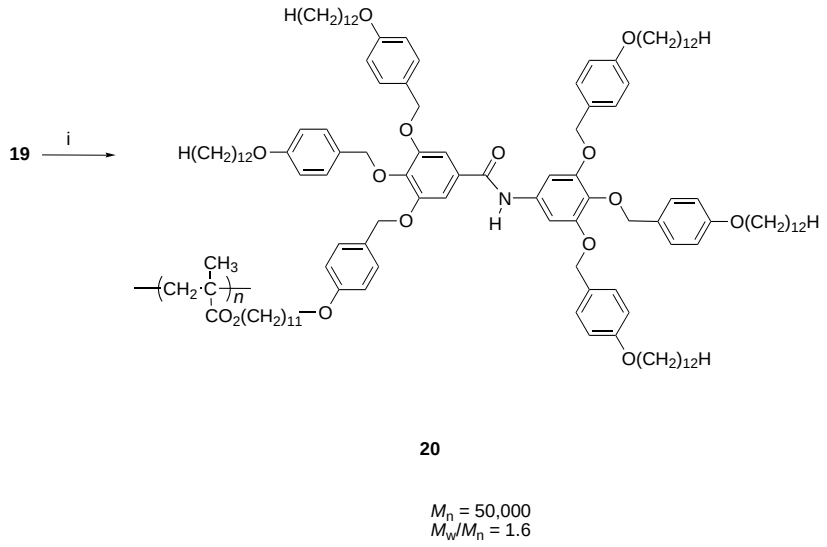

Scheme 5. i) Benzene, AIBN, 60 °C, 93 %.

The stack was subjected to energy minimization by using a MM2 molecular force field without enforcing periodic boundary conditions along the stack. By replacing the C_{12} chain with a methyl group, the calculated diameter of the rigid aromatic region of a cylinder formed by **10**, is 28.2 Å. Compound **10** forms hydrogen bonds between the amide groups along the center of the stack at a distance in the range of 1.9–2.2 Å (Figure 2, mid left). It was further found that the stack does not form a very regular cylinder of molecules, like in a crystal, but has some deviation from the crystallike order in terms of the intermolecular separation, and the orientation of similarly oriented molecules. This disorder is indicative of the liquidlike short-range order along the cylinders present in a 2D Φ_h LC phase. The average separation of similarly oriented molecules **10** in this stack is 7.2 Å.

The lattice parameter of the Φ_h phase of **10** is $a = 34.1$ Å (Figure 2, bottom). This value is significantly smaller than the length of **10**, 56.5 Å, which has a fully extended all-*trans* conformation of its alkyl tails. This difference is due to the shrinkage of alkyl tails through a mixture of *trans* and *gauche* conformers in the Φ_h LC phase.[4i] The measured cylinder diameter, 34.1 Å, shows that there is a 76 % reduction in the all-*trans* length of the alkyl tails in the LC phase. The number of molecules (μ) within a 7.2 Å stratum of the cylinder, calculated from the experimental density (ρ_{20}) of **10** and its diameter, determined by XRD, is 2.2 (Table 2). Thus, a single cylinder is formed by the criss-cross stacking of twin-dendritic benzamide **10** along the center of the cylinder by the

Table 1. Thermal characterization of **10**, **19**, **20**, and of the binary mixtures of **20** with **10** by DSC.

20/10	Phase transitions [°C] and corresponding enthalpy changes [kcal mol^{-1}]	
mol/mol	Heating[a]	Cooling[a]
100/0	*k* 64 (2.3) *k* 119 (0.15) N_c 163 (1.0) *i* *k* 56 (1.8) N_c 171[b] *i*	*i* 162[b] N_c 54 (2.0) *k*
90/10	*k* 73 (1.2) *k* 112 (0.17) N_c 164 (0.6) *i* *k* 57 (5.0) N_c 173[b] *i*	*i* 163[b] N_c 48 (2.16) *k*
80/20	*k* 70 (1.2) *k* 108 (0.25) Φ_h 165 (1.2) *i* *k* 53 (5) Φ_h 177[b] *i*	*i* 166[b] Φ_h 46 (2.0) *k*
70/30	*k* 66 (2.8) *k* 106 (0.3) Φ_h 166 (1.03) *i* *k* 67 (5.7) Φ_h 153[b] *i*	*i* 136[b] Φ_h 45 (1.62) *k*
60/40	*k* 83 (3.2) *k* 102 (0.34) $\Phi_{r\text{-}s}$ 166 (1.2) *i* *k* 84 (4.5) $\Phi_{r\text{-}s}$ 159[b] *i*	*i* 146[b] $\Phi_{r\text{-}s}$ 70 (2.5) *k*
50/50	*k* 87 (6.0) $\Phi_{r\text{-}c}$ 168 (1.1) *i* *k* 73 $\Phi_{r\text{-}c}$ 176[b] *i*	*i* 168[b] $\Phi_{r\text{-}c}$ 70 (2.0) *k*
40/60	*k* 90 (7.8) $\Phi_{r\text{-}c}$ 170 (1.34) *i* *k* 61 (2.2) $\Phi_{r\text{-}c}$ 167[b] *i*	*i* 156[b] $\Phi_{r\text{-}c}$ 67 (3.8) *k*
30/70	*k* 93 (8.9) Φ_h 173 (1.3) *i* *k* 60 (3.5) Φ_h 165[b] *i*	*i* 152[b] 66 (1.7) *k*
20/80	*k* 95 (9.9) Φ_h 173.5 (1.66) *i* *k* 90 (0.5) Φ_h 149 (0.67) *i*	*i* 145 (0.92) Φ_h 71 (0.6) *k*
10/90	*k* 98 (11) Φ_h 175 (1.85) *i* *k* 75 (−5) *k* 94 (5.5) Φ_h 161 *i*	*i* 156 (0.8) Φ_h 72 *k*
0/100	*k* 103 (13) Φ_h 178 (1.75) *i* *k* 60 (−8) *k* 100 (11) Φ_h 172 (1.66) *i*	*i* 169 (1.63) Φ_h 73 (0.8) *k*
19	*k* 57 (20.8) *k* 93 (11) Φ_h 163.5 (2.0) *i* *k* 92 (10.5) Φ_h 160.5 (1.53) *i*	*i* 156 (1.4) Φ_h 53 (9.0) *k*

[a] Data from the first heating and cooling scans are on the first line. Data from the second heating scan are on the second line. [b] Determined by TOPM as onset temperature of phase transition; *k* = crystalline, N_c = nematic columnar, *i* = isotropic, Φ_h = hexagonal columnar, $\Phi_{r\text{-}s}$ = simple rectangular columnar, $\Phi_{r\text{-}c}$ = centered rectangular columnar.

formation of the hydrogen bonds. The alkyl chains shrink to fill the space around the twin-tapered aromatic core, and produce the well-defined cylinder, which self-organizes into the 2D hexagonal columnar lattice (Figure 2, bottom). This model is similar to that previously reported for a related twin-dendritic benzamide.[4i, 15]

Structural analysis of twin-dendritic monomer 19: The diffraction pattern of monomer **19** shows sharp peaks that

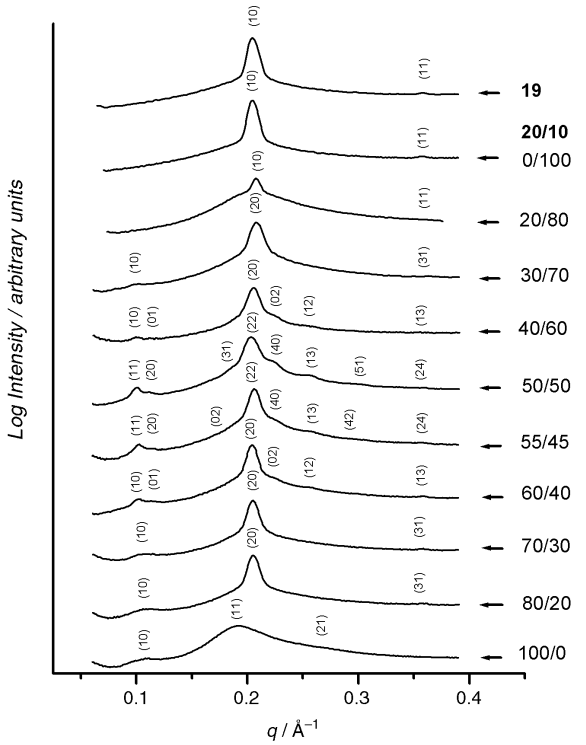

Figure 1. XRD patterns of **10**, **19**, **20**, and of **20/10** mixtures (mol/mol^{-1}).

are nearly identical to those observed in the diffraction pattern of **10** (Figure 1). Thus, compound **19** forms a 2D Φ_h LC phase with a column diameter of $a = 35.4$ Å at $T = 98$ °C. The diameter of the supramolecular cylinder generated from **19** is nearly identical to that of the cylinder generated from **10**. However, the intensity of the diffuse scattering is, interestingly, much smaller relative to that of the sharp (10) peak. Hence, the molecular organization within the supramolecular cylinders generated from **19** must be similar to that within the supramolecular cylinders generated from **10**, except for the difference in the feature that gives rise to the diffuse scattering around the strong (10) peak. Similarly, this diffuse scattering arises from dynamic rather than static disorder.

Table 2. XRD data for **19**, **10**, **20**, and for the binary mixtures of **20** with **10**.

	LC phase (T [°C])	Peak *d* spacings [Å] and their indices[a]					a [Å][b]	D_{col}[Å][c]	Rhombic unit cell surface area [Å^2][d]	ρ [g cm^{-3}]	μ[e]
		d_{10}	d_{11}	d_{20}	d_{21}	d_{31}					
10	Φ_h(94)	29.2 (s) [f]	17.2 (vw)	–	–	–	34.1 ± 0.5	34.1 ± 0.5	1007	0.93	2.2
19	Φ_h(98)	30.7 (s)	17.6 (vw)	–	–	–	35.4 ± 0.2	35.4 ± 0.2	1085	–	–
20	N_c(86)	57.1 (w,b)	32.6 (s,b)	–	24.6 (v,b)	–	65.6 ± 0.5	65.6 ± 0.5	3727	0.84	6.8
20/10 (80:20)	Φ_h(127)	58.2 (w,b)	–	30.6 (s)	–	17.4 (vw)	70 ± 3	35.1 ± 0.4	4244	–	–
20/10 (70:30)	Φ_h(128)	58.2 (w,b)	–	30.7 (s)	–	17.5 (vw)	72 ± 2	35.2 ± 0.5	4490	–	–
20/10 (30:70)	Φ_h(115)	62.8 (w,b)	–	30.2 (s)	–	17.3 (vw)	71 ± 2	34.7 ± 0.2	4366	0.91	2.1
20/10 (20:80)	Φ_h(115)	30.2 (s)	17.4 (vw)	–	–	–	34.8 ± 0.1	34.8 ± 0.1	1049	–	–

[a] The *d* spacing ratios are as expected for the 2D hexagonal columnar lattice, $d_{10}:d_{11}:d_{20}:d_{21}:d_{31} = 1:(1/\sqrt{3}):(1/2):(1/\sqrt{7}):(1/\sqrt{13})$. [b] a = lattice dimension. [c] D_{col} = column diameter. [d] Surface area of the rhombic unit cell of the 2D hexagonal lattice is given by $(a^2\sqrt{3})/2$. [e] Number of molecules occupying a single column over a 7.2 Å stratum. [f] s: strong, w: weak, vw: very weak, b: broad.

0947-6539/03/0904-0926 $ 20.00+.50/0 *Chem. Eur. J.* **2003**, *9*, No. 4

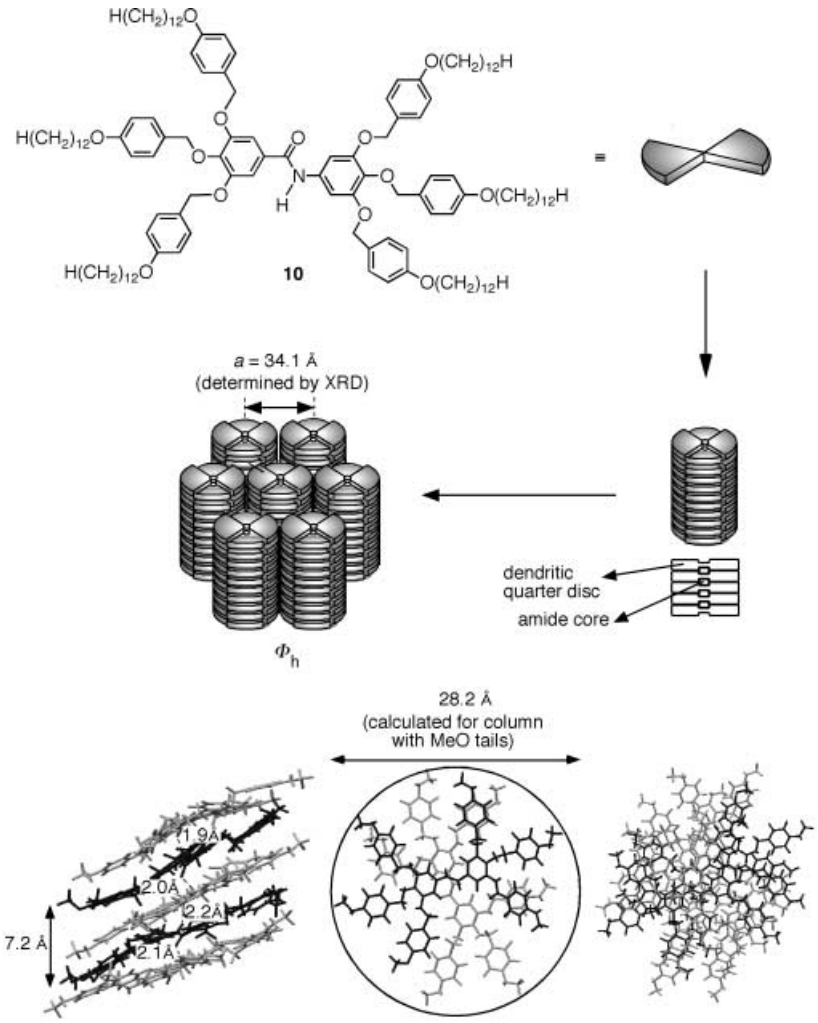

Figure 2. Schematic representation of the self-assembly of **10** into supramolecular cylindrical dendrimers that self-organize in a Φ_h lattice. The surface of the supramolecular cylinder is liquidlike. The exaggerated order of the supramolecular cylinder is shown to illustrate the mechanism of self-assembly. This schematic pattern is used in all figures of this manuscript.

Structural analysis of polymer 20: In contrast to **10** and **19**, polymer **20** shows only very broad peaks in the XRD pattern. In the diffraction pattern of **20**, a strong peak with $d = 32.6$ Å ($q = 0.193$ Å^{-1}), a weak peak with $d = 57.1$ Å ($q = 0.110$ Å^{-1}), and a very weak peak with $d = 24.6$ Å ($q = 0.255$ Å^{-1}) are observed (**20**/**10** (100:0) in Figure 1; Table 2). These peaks were indexed to the (11), (10), and (21) reflections of a 2D hexagonal lattice as their ratio is $d_{10}:d_{11}:d_{21} \approx 1:(1/\sqrt{3}):(1/\sqrt{7})$. The broadness of the peaks indicates that this 2D hexagonal lattice has only short-range structural order. These peaks did not sharpen, even after long annealing at high temperature, suggesting that their broadness is intrinsic to the structure of the LC phase. This behavior is also consistent with the texture observed by TOPM, which suggests that **20** forms a columnar nematic (N_c) phase. A characteristic texture of the N_c phase of **20** is shown in Figure 3.

The average lattice dimension a, calculated from the peak-positions of **20**, is 65.6 Å. This value is slightly smaller than double of the corresponding values for **10** and **19** in their Φ_h phase (Table 2). The a value of **20** is also significantly larger than the molecular diameter calculated for a supramolecular cylinder self-assembled with fully-extended alkyl tails. Further, and more importantly, the high intensity of the (11) peak of **20** suggests that this polymer self-assembles with its polymer backbone in the core of the cylinder. In other words, the interior region of the cylinder contains aliphatic segments of its twin-tapered dendritic side-groups, surrounding one or more polymer backbones in the central region. The exterior of the cylinder contains only aliphatic tails fanning out from the twin-tapered dendritic side groups, with the space between the exterior, and interior occupied by the aromatic region. Hence, the polymer backbone drives the formation of a *vesicular* arrangement of the molecules in a cylinder that subsequently self-organize into an N_c phase with short-range hexagonal arrangement (Figure 4). It can now be seen that the (10) peak in the diffraction pattern of **20** arises due to the polymer backbone segregated in the core of the vesicular supercylinders.

It may be noted that the experimental density of polymer **20** ($\rho_{20} = 0.84$ g cm^{-3}, Table 2) is lower than that of the twin-tapered dendrimer **10** ($\rho_{20} = 0.93$ g cm^{-3}). Since polymer **20** has short-range hexagonal arrangement in the N_c phase, its unit cell is the same as the rhombic unit cell of the hexagonal lattice. The surface area of the unit cell is $\sqrt{3}a^2/2$, in which a is the lattice dimension.

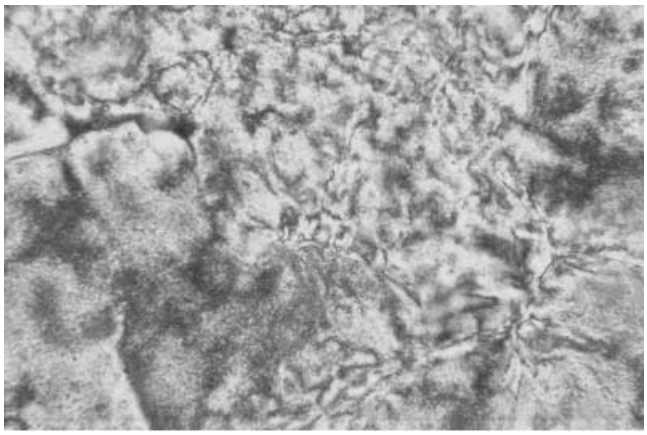

Figure 3. Optical polarized micrograph of the N_c mesophase of **20** observed at 32 °C on cooling with 0.5 °C min^{-1} from isotropic melt.

  0947-6539/03/0904-0927 $ 20.00+.50/0

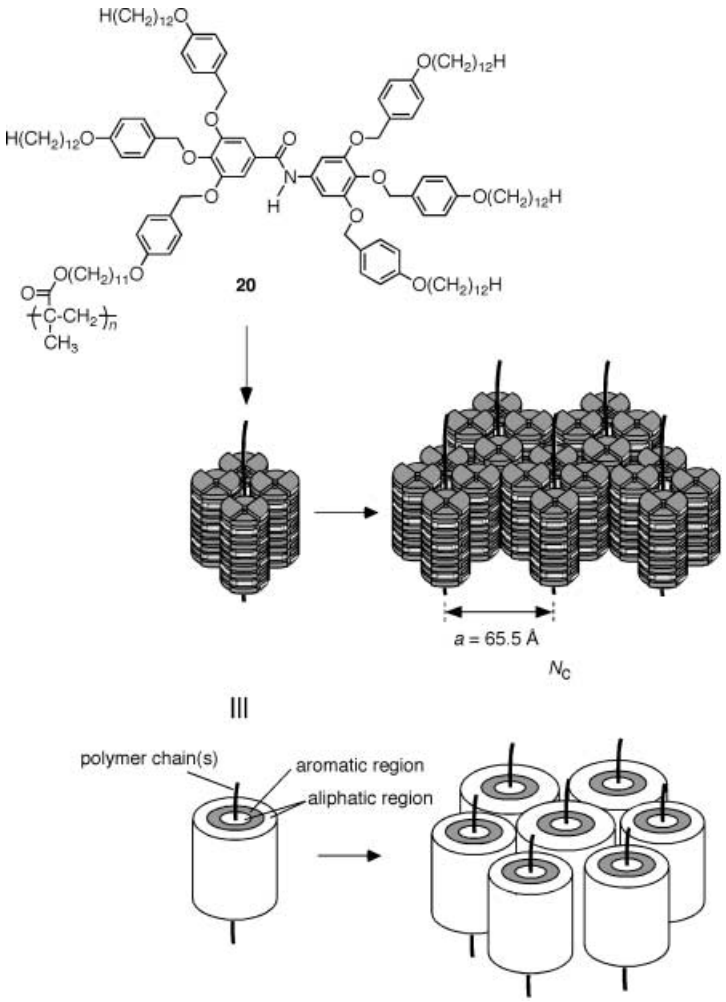

Figure 4. Schematic representation of the self-assembly of **20** into giant supramolecular cylindrical dendrimers generated from imperfect four-cylinder-bundle supramolecular dendrimers that self-organize in a N_c liquid crystalline phase with short-range hexagonal order.

In a previous study of a polymer with the same backbone, but with smaller twin-dendritic side groups, one superlattice and one sublattice reflection were observed in the XRD pattern. These reflections were indexed as (10) and (20).[4i] This is in contrast to the (10), (11), and (21) reflections observed from the present polymer **20**. Based on the XRD features, and the above discussion, it is proposed that polymer **20** exhibits the novel type of *vesicular* N_c phase shown in Figure 4. This supramolecular structure is based on a four-cylinder bundle, with one or more polymer backbones in the interior, and can pack into an N_c phase with short-range hexagonal order. Therefore, a larger cylinder consisting of more than one polymer backbone segregated in the center and surrounded by a bundle of four polymeric cylinders is produced (Figure 4).

Structural analysis of binary mixtures of polymer 20 with twin-dendritic benzamide 10: Binary mixtures of **20** with **10** (**20**/**10** (*x*:*y*) where *x*:*y* = mol mol^{-1} ratio of the repeat unit of **20** with **10**) were prepared in THF and dried at 20 °C under vacuum. The thermal transitions and their corresponding enthalpy changes are summarized in Table 1. All binary mixtures exhibit homogeneous isotropizations with corresponding transition temperatures lying between that of the parent components **20** and **10**.

A Φ_h LC phase is formed by mixtures containing more than 70 mol % of **10**. Mixtures containing less than 20 mol % of **10** form an N_c phase (Table 2), and therefore, behave similarly to the pure polymer **20**. Mixtures of **20**/**10** containing between 20 and 70 mol % of **10** exhibit several new phases. Their structure is dictated by the amount of **10** present in the **20**/**10** mixture.

Analysis of 20/10 (80:20 and 70:30): Mixtures containing 20 and 30 mol % of **10** show one strong sharp peak at $d = 30.6$ Å ($q = 0.205$ Å^{-1}) and a very weak sharp peak at $d = 17.1$ Å ($q = 0.367$ Å^{-1}) (Table 2, Figure 1). In addition, **20**/**10** (80:20) and **20**/**10** (70:30) compositions show a broad peak of low intensity at $d = 58.2$ Å ($q = 0.108$ Å^{-1}). The d spacings of these peaks, 58.2, 30.6, and 17.1 Å are in the ratio (1):(1/2):(1/$\sqrt{13}$). This ratio corresponds to the d_{10}, d_{20}, and d_{31} reflections of a 2D hexagonal lattice, and, therefore, this is a 2D Φ_h LC phase.

The surface area of the rhombic unit cell of polymer **20** (3727 Å^2) is 3.7 times larger than that of the twin-dendritic molecule **10** (1007 Å^2). This indicates that nearly four twin-dendritic cylinders occupy the rhombic unit cell of polymer **20**. The number of repeat units of **20** that occupy a 7.2 Å stratum of a single rhombic unit cell of the short-range hexagonal arrangement of the N_c phase, calculated using the experimental density ($\rho_{20} = 0.84$ g cm^{-3}) and the lattice dimension ($a = 65.6$ Å), is 6.8 (Table 2). An attempt to arrange the molecules of the twin-tapered dendrimer **10** into the rhombic unit cell, with the same dimension as that of polymer **20**, but with the density of **10** ($\rho_{20} = 0.93$ g cm^{-3}), yields a value of 7.5. This value is higher than the 6.8 repeat units of polymer **20** that are contained in the same unit cell. These results show that there is some amount of empty space in the supramolecular cylinders that form the N_c phase of the polymer **20** as indicated by the white layers of the cylinders in Figure 4. Therefore, this polymer has three different structural disorders: the polymer backbone region located between the supramolecular cylinders, the position of these cylinders, and the empty space within them.

0947-6539/03/0904-0928 $ 20.00+.50/0 *Chem. Eur. J.* **2003**, *9*, No. 4

These mixtures also show diffuse scattering centered nearly at the same position as the sharp strong peak observed in the Φ_h phase of **10** (Figure 1). Therefore, the observed diffraction pattern of **20**/**10** (80:20 and 70:30) is very similar to that of **10** except for the broad (10) peak at $q = 0.108$ Å^{-1} ($d = 58.2$ Å). The position and width of the broad peak in these mixtures is almost the same as that observed in polymer **20**. The appearance of the sharp peaks in these **20**/**10** mixtures are almost in the same position as in the case of the twin-tapered dendritic molecule **10**, and their very similar widths suggest that the twin-tapered dendritic side groups of the polymer molecule self-assemble *easier* in the presence of the twin-tapered dendritic molecules **10**. Therefore, the side-groups of **20** must co-assemble with **10**, which is similar in size to the missing side groups of **20** and fills the empty space in the imperfect four-cylinder-bundle supramolecular dendrimer that results from **20** (Figure 5). Therefore, during this process **20** acts as a host and **10** as a guest, and their mixtures produce host–guest complexes. When all the empty guest places of **20** are filled with **10**, the imperfect four-cylinder-bundle **20** becomes a perfect four-cylinder-bundle supramolecular dendrimer. Subsequently, the self-organization of the four-cylinder-bundle of **20**/**10** (80/20 and 70/30) mixtures forms a Φ_h superlattice with a lattice dimension $a = 70$ Å and 72 Å, respectively. In this superlattice, the polymer backbones occupy the core of the four-cylinder-bundles, and the twin-tapered dendritic molecules **10** correct the structural defects, such as, empty spaces of the disordered bundle of pure **20** (Figures 4 and 5). Also, correcting these structural defects enables the side-groups of the polymer **20** to form well-ordered individual cylinders through the host–guest complexes described above. However, the near equivalence of the (10) peak to that seen in polymer **20** demonstrates that the polymer backbone region of the supramolecular cylinder continues to be as disordered as in the parent **20**. A top view of the Φ_h superlattice, formed by the polymer backbone bundles of these mixtures, and the subcells formed by the twin-dendritic cylinders are shown in Figure 6a.

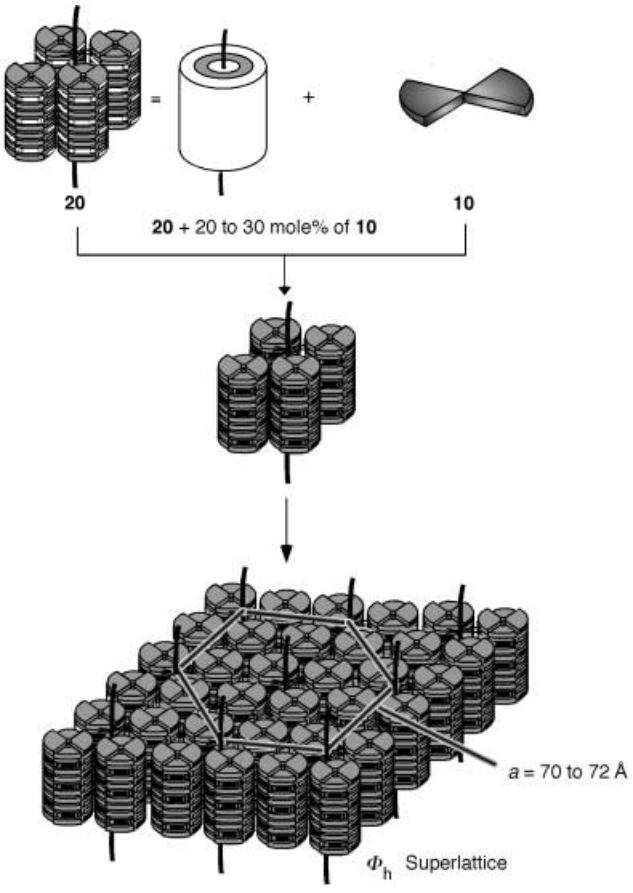

Figure 5. Schematic representation of the co-assembly of binary mixtures **20**/**10** (80:20 to 70:30) into perfect four-cylinder-bundle supramolecular dendrimers that self-organize in a Φ_h superlattice.

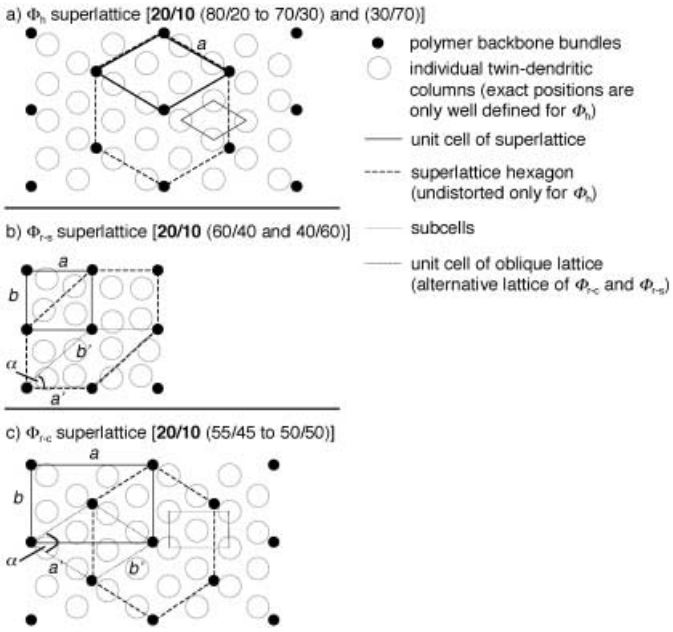

Figure 6. Top views of the cross-sections of the superlattices formed by binary mixtures **20**/**10** (80:20 to 40:60).

Analysis of 20/10 (60:40): There are two narrower peaks for the mixture **20**/**10** (60:40) in the $q \approx 0.1$ Å^{-1} region. This is in contrast to the single broad peak observed in the same region for **20**/**10** (70:30). Similarly, in the $q \approx 0.2$ Å^{-1} region, there are two slightly broader peaks rather than a single sharp peak for the mixture **20**/**10** (60:40). In addition, two slightly broader weak peaks appear at $q = 0.224$ Å^{-1} ($d = 28.1$ Å), and $q = 0.252$ Å^{-1} ($d = 24.9$ Å), respectively. For the same mixture, there is a very strong peak at $q = 0.204$ Å^{-1} (30.8 Å), and a weak peak at $q = 0.357$ Å^{-1} (17.6 Å). These two peaks occur at almost the same position as those observed for the mixture **20**/**10** (70:30). All the peaks could be indexed to a simple rectangular superlattice $\Phi_{r\text{-}s}$ with the dimensions $a = 61.4$ Å and $b = 55.1$ Å (Figure 6b). Thus, the peak with $q = 0.108$ Å^{-1} indexed as (10), in the case of **20**/**10** (80:20 to 70:30), becomes two peaks in **20**/**10** (60:40) with the indices (10) and (01). The index for the most intense peak is (20) and for the peak at $q = 0.224$ Å^{-1} is (02). The (20) and (02) peaks are the second order peaks arising from (10) and (01), respectively. The fact that the (20) peak is stronger than the (10) peak and appears at

  0947-6539/03/0904-0929 $ 20.00+.50/0

almost the same position as the (10) peak observed in the twin-dendrimer **10**, suggests that the shapes of the individual supramolecular cylinders forming the $\Phi_{r\text{-}s}$ phase are very similar to those of the twin-dendrimer **10** in its Φ_h phase. However, in this **20/10** (60:40) mixture (Figure 6b), the average position of the centers of the individual cylinders vary slightly from one unit cell to another. The ratio $a/b = 1.11$ shows it is only slightly distorted from being a simple square lattice. Alternatively, this structure can be considered as an oblique lattice, with $a' = 61.4$ Å, $b' = 82.5$ Å, and an included angle of $\alpha = 41.9^\circ$ (thin dotted line in Figure 6b). It should be noted that the lattice dimensions of the $\Phi_{r\text{-}s}$ superlattice ($a =$ 61.4 Å and $b = 55.1$ Å) are only slightly different from the diameter of the supercylinder (65.6 Å) formed in the N_c phase of polymer **20**. This shows that the four-cylinder-bundles of the polymer self-organize into the $\Phi_{r\text{-}s}$ lattice upon the addition of 40 mol% of **10**, which induces changes in the relative positions of the supramolecular cylinders of the dendritic units surrounding the polymer backbone. This change favors a simple rectangular arrangement rather than a hexagonal one, which is preferred by the pure polymer **20** in the N_c phase, as well as by the mixtures **20/10** (80:20 to 70:30) in the superlattice LC phase.

Analysis of 20/10 (55:45 and 50:50): The **20/10** mixtures containing from 45 to 50 mol% of **10** (i.e., **0/10** (55:45 to 50:50)) exhibit more diffraction peaks than the mixtures containing 40 mol% of **10** (i.e., **20/10** (60:40), Table 3, Figure 1). The intensity of the additional peaks increases as the concentration of **10** increases from 45 to 50 mol%. We discuss the diffraction results for **20/10** (50:50), since its peaks are most prominent in the XRD pattern. The diffraction pattern of **20/10** (50:50) shows two close peaks at $q \approx 0.1$ Å^{-1} ((11) and (20) in Figure 1), which are narrower than the single broad (10) peak observed in **20/10** (70:30). The peak positions of **20/10** (50:50) are indexed to a centered rectangular ($\Phi_{r\text{-}c}$) superlattice with dimensions $a = 113.5$ Å and $b = 73.8$ Å (Figure 6c). The indices for the peaks with $q \approx 0.1$ Å^{-1} are (11) and (20), and the most intense peaks are indexed as (22) and (40). These most intense peaks occur nearly at the same position as the strong (10) peak observed for **10**. The (22) and (40) peaks are the second order peaks arising from (11) and (20) peaks respectively. Similar to **20/10** (60:40), the (22) peak is stronger than the (11) peak and appears at almost the same position as the (10) peak of **10**; this leads again to the conclusion that the individual supramolecular cylinders forming the $\Phi_{r\text{-}c}$ phase are very similar to those of the twin-dendrimer **10** in its Φ_h phase. The ratio of the centered rectangular lattice dimensions a/b is 1.54. This value is close to the value $\sqrt{3}$, expected for an undistorted hexagonal lattice indexed to a centered rectangular lattice. Alternatively, this structure can be considered as an oblique lattice with $a' = b' = 67.7$ Å and an included angle of $\alpha = 66.1^\circ$ (thin dotted line in Figure 6c). The angle $\alpha = 66.1^\circ$ corresponds to only a slight distortion of $\alpha = 60.0^\circ$ which is the ideal value for an undistorted hexagonal lattice. In other words, the $\Phi_{r\text{-}c}$ superlattice of **20/10** (55:45 to 50:50) can be considered as the distorted version of the columnar hexagonal superlattice, exhibited by **20/10** (80:20 and 70:30).

Analysis of 20/10 (40:60): The diffraction pattern of the mixtures **20/10** (40:60) is very similar to that of **20/10** (60:40). Thus, all the peaks were indexed to a simple rectangular superlattice ($\Phi_{r\text{-}s}$; Figure 6b with the lattice dimensions $a =$ 60.9 Å and $b = 54.9$ Å, with the same indices for the corresponding peaks. Therefore, the supramolecular self-organization is very similar to that for the mixture **20/10** (60:40).

Analysis of 20/10 (30:70): Most of the reflections observed in **20/10** (60:40 to 40:60) are not observed in **20/10** (30:70) (Table 2, Figure 1). Instead **20/10** (30:70) exhibits only a single broad peak at $q = 0.100$ Å^{-1} ((10) peak for 30:70 mixture in Figure 1), at nearly the same position as that observed in **20/10** (60:40 to 40:60). However, the (10) peak of **20/10** (30:70) becomes narrower and is shifted towards lower q values than the (10) peak observed in the same region for the mixtures of **20/10** (80:20 and 70:30), as well as for the polymer **20** (**20/10** (100:0) in Figure 1). In addition to the broad (10) peak, **20/10** (30:70) shows sharp peaks at $q = 0.208$ Å^{-1} and $q = 0.363$ Å^{-1}. They are nearly at the same position as those observed in **20/10** (70:30). The $d_{10} = 62.8$ Å ($q = 0.100$ Å^{-1}) peak of **20/10** (30:70) is about 7% larger than the d spacing of the (10) peak of **20/10** (70:30), and is also narrower. This suggests that the

Table 3. XRD data for the binary mixtures of the polymer **20** with **10** in the centered rectangular columnar ($\Phi_{r\text{-}c}$) and simple rectangular columnar ($\Phi_{r\text{-}s}$) LC phases.

	LC phase (T [°C])	Peak d spacings [Å] and their indices										a and b[c] [Å]	ρ [g cm^{-3}]	μ[d]
		d_{10}[a] d_{11}[b]	d_{01}[a] d_{20}[b]	d_{02}[b]	d_{31}[b]	d_{20}[a] d_{22}[b]	d_{02}[a] d_{40}[b]	d_{12}[a] d_{13}[b]	d_{42}[b]	d_{51}[b]	d_{13}[a] d_{24}[b]			
20/10 (60:40)	$\Phi_{r\text{-}s}$[e] (115)	62.2	55.1	–	–	30.8	28.1	24.9	–	–	17.6	$a = 61.4$ $b = 55.1$	–	–
20/10 (55:45)	$\Phi_{r\text{-}c}$[f] (121)	62.2	55.1	36.7	–	30.5	28.8	24.5	22.3	–	17.7	a = 113.0 $b = 74.3$	0.91[g]	2.1
20/10 (50:50)	$\Phi_{r\text{-}c}$[f] (121)	62.8	56.1	–	33.6	30.8	28.6	24.5	–	21.7	17.5	$a = 113.5$ $b = 73.8$	0.91	2.0
20/10 (40:60)	$\Phi_{r\text{-}s}$[e] (121)	62.2	54.6	–	–	30.7	28.1	24.5	–	–	17.6	$a = 60.9$ $b = 54.9$	--	–

[a] d spacings with indices for simple rectangular columnar LC superlattice ($\Phi_{r\text{-}s}$). [b] d spacings with indices for centered rectangular columnar LC superlattice ($\Phi_{r\text{-}c}$). [c] Lattice dimensions. [d] Number of molecules occupying a single column over a 7.2 Å stratum. [e] For the simple rectangular lattices reported here, the d spacing ratios are (within 2%): $d_{10}:d_{01}:d_{20}:d_{02}:d_{12}:d_{13} = 1.00:(1/1.13):(1/2.02):(1/2.22):(1/2.50):(1/3.54)$. [f] For the centered rectangular lattices reported here, the d spacing ratios are (within 2%): $d_{11}/d_{20}/d_{02}/d_{31}/d_{22}/d_{40}/d_{13}/d_{51}/d_{24} = 1.00:(1/1.09):(1/1.67):(1/1.83):(1/1.99):$ $(1/2.18):(1/2.56):(1/2.84):(1/3.51)$. [g] The density is assumed to be 0.91 g cm^{-3}, since the measured density for the mixtures containing 50 mol% and 70 mol% of **10** are the same.

0947-6539/03/0904-0930 $ 20.00+.50/0 *Chem. Eur. J.* **2003**, *9*, No. 4

lower concentration of polymer **20** in **20**/**10** (30:70) increases the average distance between the polymer backbone bundles. The regions occupied by the polymer backbone are less disordered than in the mixtures containing larger amounts of **20**. It is conceivable that the number of polymer strands varies along the center of the supramolecular cylinders (Figure 7b) resulting in regions of empty space that are filled by short stacks of twin-dendritic benzamide **10** (Figure 7a). Thus, the mixture **20**/**10** (70:30) forms a Φ_h superlattice with a lattice dimension double that of the pure **10**. Alternatively, this can be viewed as a result of displacing one or two polymer strands along the center of the supramolecular cylinders by a certain distance, which would create empty regions in the cylinders that can be filled by short stacks of **10**. At low enough concentrations of polymer **20**, this can give rise to the repeat units of the polymer **20** occupying only three neighboring columns surrounding the backbones (Figure 7c).

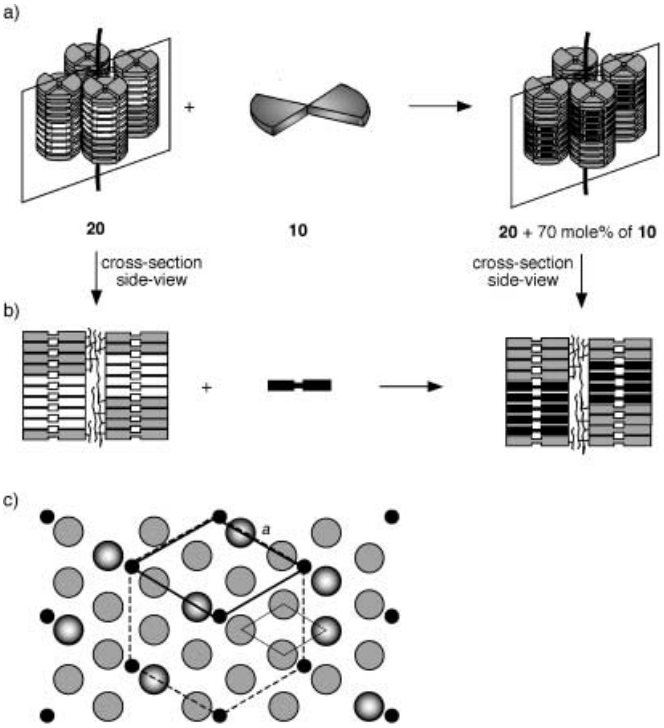

Figure 7. Schematic representation of the self-assembly of binary mixtures **20** (30:70) into a Φ_h superlattice, either by maintaining the four-cylinder-bundle supramolecular dendrimers, but with having larger regions of **10** in the individual cylinders (a/b) or by a combination of a three-cylinder-bundle supramolecular dendrimer polymer and non-uniformly distributed individual dendritic cylinders (c).

Analysis of 20/10 (20:80): Once the concentration of the twin-tapered dendrimer **10** in the mixture reaches 80 mol% (i.e. **20**/**10** (20:80)), we no longer observe any features in the $q \approx 0.1$ Å^{-1} region. Only two sharp peaks at $q = 0.208$ Å^{-1} and $q = 0.361$ Å^{-1} are observed. They are at almost the same position as in the case of the twin-tapered dendrimer **10**. The polymer **20** concentration is insufficient to form an ordered superlattice, and, therefore, we assume that this mixture forms a 2D Φ_h lattice similar to that of pure **10**, but with a nonuniform distribution of polymer **20**, which is very similar in size and shape to **10**, and replaces **10** in its lattice. Since polymer **20** does not form any ordered superlattice structure, it destabilizes the isotropization temperature of the mixture **20**/**10** (20:80) by 24.5 °C during the second heating scan of the DSC (Table 1).

In summary, the LC phase behavior of the binary mixtures of the polymer **20** with the twin-tapered dendritic benzamide **10** (**20**/**10** (x:y)) follows the composition trend shown in Figure 8: for $y < 20$: N_c, $20 \le y \le 30$: Φ_h superlattice, formed by four-cylinder-bundle supramolecular dendrimer **20**; for $30 < y < 45$: $\Phi_{r\text{-}s}$ superlattice, formed by distorted four-cylinder-bundle supramolecular dendrimer **20**; for $45 \le y < 60$: $\Phi_{r\text{-}c}$ superlattice; for $60 \le y < 70$: $\Phi_{r\text{-}s}$ superlattice; for $70 \le y < 80 <$: Φ_h superlattice, and for $y \ge 80$ Φ_h lattice with no superlattice ordering.

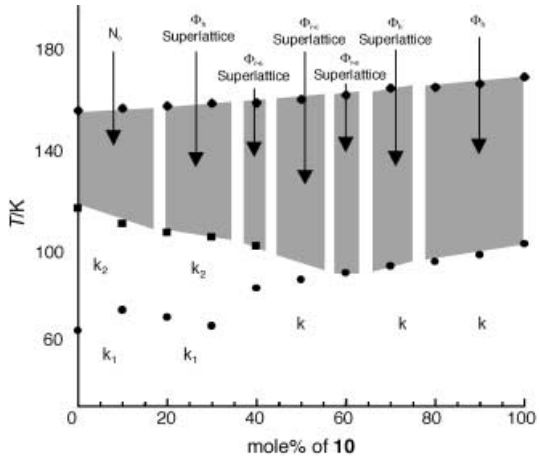

Figure 8. Hierarchical formation of lattices and superlattices self-organized and co-organized from the supramolecular architectures generated from **10**, **20**, and from mixtures **20**/**10** (x:y) and their thermal stability range.

Conclusion

The twin-dendritic benzamide **10** self-assembles into supramolecular cylinders that self-organize in a Φ_h lattice. The same twin-tapered dendritic molecules attached to a polymethacrylate backbone (**20**) and self-assemble into an imperfect four-cylinder-bundle supramolecular dendrimer that forms a novel giant *vesicular* supercylinder that self-organizes in a N_c phase with short range hexagonal order. The imperfect four-cylinder-bundle supramolecular dendrimer **20** serves as a host to form long-range ordered hexagonal and different types of rectangular columnar 2D superlattices when it is mixed with **10**, which acts as a guest. The host–guest complex of **20** with **10** generates a perfect four-cylinder-bundle supramolecular dendrimer. The Φ_h superlattice contains disordered regions of segregated polymer backbones, while the $\Phi_{r\text{-}s}$ and $\Phi_{r\text{-}c}$ superlattices contain less disordered regions of segregated polymer backbones. The nature of the superlattices formed is determined by the concentration of **10** in the **20**/**10** mixtures. The concept used to generate these novel superlattices can be elaborated to design novel functional and complex ordered soft condensed matter with potential applications in surface

nanopatterning, membranes, nanoelectronics, and molecular-recognition-based processes. In addition, the twin-dendritic benzamide concept based on two identical tapered dendrons can be extended to benzamides based on dissimilar tapered and other dendritic shapes. Research along this line is in progress in our laboratory.

Experimental Section

Materials: 11-Bromoundecanoic acid (99%), methyl-4-hydroxybenzoate (99%), 1,2,3-trimethoxybenzene (98%), methyl-3,4,5-trihydroxybenzoate (98%), $SOCl_2$ (99%), $LiAlH_4$ (95%), pyridine (99%), graphite, Amberlite-120 (all from Aldrich), borane-THF complex (1.0 M solution), 1-bromododecan (98%), hydrazine hydrate (98%), triethyl orthoformate (98%), catechol (99%), 3,4-dihydroxybenoic acid (97%), K_2CO_3 (99%), $MgSO_4$, DMF (Lancaster), HCl, H_2SO_4, HNO_3, KOH; Na_2SO_4, $NaHCO_3$ (Fisher), methacryloyl chloride (97%) (Acros), silica gel (Natland) were used as received. The nitrating agent (25% HNO_3 on silica gel by titration with 1*N* NaOH using phenolphthalein as an indicator) was prepared according to a literature procedure,[16] and was used after drying in air for seven days. Benzene (thiophene-free, Fisher) used for the free radical polymerizations was washed three times with concentrated H_2SO_4 and dried over $MgSO_4$. 4′-Dodecyloxybenzyl chloride (**4**) and 4′-(11′-hydroxyundecyloxy)benzylchloride (**12**) were synthesized according to literature procedures.[5n]

Techniques: ^{1}H (200 MHz) NMR spectra were recorded on a Bruker AC-200. ^{13}C (90 MHz, 125 MHz) NMR spectra were recorded on a Bruker AC-360 and Bruker DRX 500. Thin layer chromatography (TLC) was performed on precoated TLC plates (silica gel with F_{254} indicator; layer thickness, 200 mm; particle size, 5 ~ 25 mm; pore size, 60 Å, SIGMA-Aldrich). Melting points were measured using a uni-melt capillary melting point apparatus, (Thomas) and are uncorrected.

GPC analysis was performed on a Shimadzu LC-10AT high pressure liquid chromatograph equipped with CTO-10A column oven (40 °C), a PE Nelson Analytical 900 Series integrator data station, Shimadzu RID-10A RI detector, SPD-10A UV-Vis detector (254 nm), and two columns AM gel (10 mm, 500 Å and 10 mm, 10^4 Å). THF (Fisher HPLC grade) was used as eluent at a flow rate of 1 mL min^{-1}. Number and weight average molecular weights were determined using calibration plots constructed with polystyrene standards.

Thermal transitions were measured on a Perkin–Elmer DSC-7 differential scanning calorimeter (DSC). In all cases, the heating and the cooling rates were 10 °C min^{-1}. The transition temperatures were reported as the maxima and minima of their endothermic and exothermic peaks. Indium was used as calibration standard. An Olympus BX-40 optical polarized microscope (100 × magnification) equipped with a Mettler FP 82 hot stage and a Mettler FP 80 central processor was used to verify thermal transitions and characterize anisotropic textures.

X-ray diffraction measurements were carried out with $Cu_{K\alpha}$ radiation from a Bruker-Nonius FR-591 rotating anode X-ray source with a 0.2×2.0 mm^2 filament operated at 3.4 kW. The beam was collimated and focused by a single bent mirror and sagitally focusing Ge(111) monochromator, resulting in a 0.2×0.2 mm^2 spot on a multiwire detector 125 cm from the sample. To minimize attenuation and background scattering, an integral vacuum was maintained along the length of the flight tube and within the sample chamber. The samples were held in a temperature-controlled (±0.1 °C) oven. Densities (ρ_{20}) were determined by flotation in gradient columns at 20 °C. Elemental analyses of all new compounds (M-H-W Laboratories, Phoenix, AZ) agree with the calculated value within ± 0.4%.

3,4,5-Trimethoxy-1-nitrobenzene (2): Compound (**1**) (40 g, 0.238 mol) in CH_2Cl_2 (100 mL) was added rapidly to a stirred suspension of $SiO_2 \cdot HNO_3$ (132 g, 0.354 mol) in CH_2Cl_2 (400 mL) at 20 °C. The resulting red solution was stirred at 20 °C for 15 min. SiO_2 was filtered and washed several times with CH_2Cl_2. The organic phases were combined, concentrated, and precipitated in MeOH. The yellow crude product was filtered and extracted with hot MeOH. Purification by column chromatography (SiO_2, EtOAc/hexane 1:4) produced 16.5 g (33%) of **2** as yellow crystals. Purity: 99% (HPLC); m.p. 98–99 °C (lit[17]: 99–100 °C); ^{1}H NMR (200 MHz, $CDCl_3$, 20 °C, TMS): $\delta = 3.94$ (s, 9H; CH_3OPh), 7.52 ppm (s, 2H; ArH).

3,4,5-Trihydroxy-1-nitrobenzene (3): Compound **2** (5 g, 23 mmol) was mixed with pyridine hydrochloride (20 g). The mixture was stirred at 200 °C for 40 min. The reaction mixture was extracted with EtOAc three times and washed with dilute HCl, H_2O, and finally with brine. The organic phase was dried over anhydrous $MgSO_4$ and evaporated to yield 2.75 g (69%) of **3** as yellow crystals. The product was used for the next reaction without further purification. M.p. 195–197 °C (194–196 °C).[18]:

3,4,5-Tris(4′-dodecyloxybenzyloxy)-1-nitrobenzene (5): Compound **3** (2.75 g, 16 mmol), K_2CO_3, and DMF (100 mL) was added to a 500 mL two-necked round bottomed flask, and N_2 was bubbled through the solution for 20 min. After the addition of **4** (15.3 g, 49 mmol), the reaction mixture was stirred at 70 °C for 24 h under N_2. The reaction mixture was cooled to 20 °C and poured into an ice-water mixture. The crude product was separated as a white solid, filtered, and dried under vacuum. The crude product was passed through a short column of silica gel using Et_2O as eluent. The obtained product was purified by column chromatography (EtOAc/hexanes 1:9) and recrystallized from acetone to obtain 11.4 g (76%) of **5** as white crystals. Purity: 99% (HPLC); m.p. 76–77 °C; $R_f = 0.65$ (hexanes/EtOAc 4:1); ^{1}H NMR (200 MHz, $CDCl_3$, 20 °C, TMS): $\delta =$ 0.88 (t, ^3J(H,H) = 6.4 Hz, 9H; CH_3,), 1.27 (overlapped m, 54H; $(CH_2)_9$, 1.77 (m, 6H; CH_2CH_2OPh), 3.95 (m, 6H; CH_2OPh), 5.06 (d, ^3J(H,H) = 2.4 Hz, 6H; $PhCH_2OPh$), 6.75 (d, 2H; *meta* to CH_2OPh, 4-position), 6.89 (d, ^3J(H,H) = 8.7 Hz, 4H; *meta* to CH_2OPh, 3,5-position,), 7.20–7.34 (m, 6H; *ortho* to CH_2OPh), 7.55 ppm (s, 2H; *ortho* to NO_2); ^{13}C NMR (90 MHz, $CDCl_3$, 20 °C, TMS): $\delta = 14.3, 22.9, 26.3, 29.7, 32.1, 68.2, 71.5, 75.1, 103.5, 114.6, 127.9–130.5, 143.0, 144.0, 152.7, 159.4$ ppm; elemental analysis calcd (%) for $C_{63}H_{95}NO_8$ M_W: C 76.08, H 9.62, N 1.40; found: C 75.93, H 9.58, N 1.46.

3,4,5-Tris(4′-dodecyloxybenzyloxy)-1-aminobenzene (6): Compound **5** (4 g, 4 mmol), $NH_2NH_2 \cdot H_2O$ (1 mL, 20 mmol), and graphite (3.5 g) were heated in refluxing EtOH (50 mL) for 24 h under Ar. The reaction mixture was cooled to 20 °C and was diluted with CH_2Cl_2 (50 mL). Graphite was filtered and washed several times with CH_2Cl_2. The colorless organic phase was concentrated and precipitated in MeOH .The solid was filtered and recrystallization from acetone produced 3.18 g (82%) of **6** as white crystals. Purity: 99% (HPLC); m.p. 84–86 °C; $R_f = 0.11$ (hexanes/EtOAc 4:1); ^{1}H NMR (200 MHz, $CDCl_3$, 20 °C, TMS): $\delta = 0.88$ (t, ^3J(H,H) = 6.4 Hz, 9H; CH_3), 1.27 (overlapped m, 54H; $(CH_2)_9$, 1.76 (m, 6H; CH_2CH_2OPh), 3.94 (m, 6H; CH_2OPh), 4.93 (d, ^3J(H,H) = 22.3 Hz, 6H; $PhCH_2OPh$), 5.99 (s, 2H; *ortho* to NH_2), 6.75 (d, ^3J(H,H) = 8.7 Hz, 2H; *meta* to CH_2OPh, 4-position), 6.87 (d, ^3J(H,H) = 8.7 Hz, 4H; *meta* to CH_2OPh, 3,5-position), 7.28 ppm (m, 6H; *ortho* to CH_2OPh); ^{13}C NMR (90 MHz, $CDCl_3$, 20 °C, TMS): $\delta = 14.3, 22.9, 26.3, 29.7, 32.1, 68.2, 71.2, 75.2, 96.0, 114.4, 129.2–131.5, 142.6, 153.7, 159.0$ ppm; elemental analysis calcd (%) for $C_{63}H_{97}NO_6$: C 78.45, H 10.13, N 1.45; found: C 78.20, H 10.47, N 1.41.

Methyl 3,4,5-Tris(4′-dodecyloxybenzyloxy)benzoate (8): Compound **8** was synthesized by using a similar procedure as the one used for the synthesis of **5**. Starting from compounds **7** (1.55 g, 8.4 mmol), **4** (7.86 g, 25.3 mmol), and K_2CO_3 (7 g, 50.7 mmol) in DMF (50 mL), 7.65 g (90%) of **8** was obtained as white crystals after recrystallization from acetone. Purity: 99% (HPLC); m.p. 67–68 °C; $R_f = 0.78$ (hexanes/EtOAc 4:1); ^{1}H NMR (200 MHz, $CDCl_3$, 20 °C, TMS): $\delta = 0.89$ (t, ^3J(H,H) = 6.1 Hz, 9H; CH_3), 1.27 (overlapped m, 54H; $(CH_2)_9$), 1.79 (m, 6H; CH_2CH_2OPh), 3.89–3.97 (overlapped m, 9H; CH_2OPh, CO_2Me), 5.05 (d, ^3J(H,H) = 7.6 Hz, 6H; $PhCH_2OPh$), 6.75 (d, ^3J(H,H) = 8.4 Hz, 2H; *meta* to CH_2OPh, 4-position), 6.89 (d, ^3J(H,H) = 8.4 Hz, 4H; *meta* to CH_2OPh, 3,5-position), 7.23–7.36 ppm, (m, 8H; *ortho* to CH_2OPh, *ortho* to CO_2Me); ^{13}C NMR (90 MHz, $CDCl_3$, 20 °C, TMS): $\delta = 14.3, 22.9, 26.3, 29.7, 32.1, 52.4, 68.2, 71.2, 74.9, 109.3, 114.6, 125.2, 128.7–130.5, 142.6, 152.8, 159.2, 166.9$ ppm.

3,4,5-Tris(4′-dodecyloxybenzyloxy)benzoic acid (9): Compound **8** (7.5 g, 7.5 mmol), EtOH (80 mL), and KOH solution (1 g dissolved in 10 mL H_2O) was placed into a 200 mL round flask containing a Teflon coated magnetic stirring bar. The mixture was refluxed for 2 h under constant stirring. The extent of reaction was followed by TLC. After the reaction was complete, the reaction mixture was cooled to 20 °C. The reaction mixture was diluted with THF (100 mL), and was acidified with dilute HCl to pH 1 at 0 °C. The reaction mixture was poured into an ice—water mixture. The precipitated white solid was collected by filtration and dried. Recrystallization of the

0947-6539/03/0904-0932 $ 20.00+.50/0 *Chem. Eur. J.* **2003**, *9*, No. 4

crude product from acetone produced 7.10 g (96%) of **9** as white crystals. Purity: 99% (HPLC); m.p. 142–143 °C; ^{1}H NMR (200 MHz, $CDCl_3$, 20 °C, TMS): $\delta = 0.88$ (t, $^3J(H,H) = 6.4$ Hz, 9H; CH_3), 1.27 (overlapped m, 54H; $(CH_2)_9$), 1.79 (m, 6H; CH_2CH_2OPh), 3.95 (m, 6H; CH_2OPh), 5.05 (d, $^3J(H,H) = 5.3$ Hz, 6H; $PhCH_2OPh$), 6.75 (d, $^3J(H,H) = 8.6$ Hz, 2H; *meta* to CH_2OPh, 4-position), 6.90 (d, $^3J(H,H) = 8.6$ Hz, 4H; *meta* to CH_2OPh, 3,5-position), 7.23–7.36 (m, 6H; *ortho* to CH_2OPh), 7.42 ppm (s, 2H; *ortho* to CO_2H); ^{13}C NMR (90 MHz, $CDCl_3$, 20 °C, TMS): $\delta = 14.3$, 22.9, 26.3, 29.7, 32.1, 68.2, 71.3, 74.9, 109.9, 114.5, 124.2, 128.6–130.5, 143.4, 152.9, 159.2, 171.8 ppm.

***N*-[3,4,5-Tris(4′-dodecyloxybenzyloxy)phenyl]-3,4,5-tris(4′-dodecyloxybenzyloxy)benzamide (10)**: Compound **9** (1.0 g, 1.0 mmol), **6** (0.97 g, 1.0 mmol), DCC (624 mg, 3.0 mmol), DPTS (89 mg, 0.3 mmol), and dry CH_2Cl_2 (20 mL) under N_2 were placed in a 50 mL three-necked round bottomed flask containing a Teflon coated magnetic stirring bar. The reaction mixture was stirred at 20 °C for 24 h. The extent of the reaction was followed by TLC. After the reaction was completed, the reaction mixture was precipitated in MeOH. The solid was collected by filtration and dried in air. Purification of the crude product by column chromatography (EtOAc/hexanes 1:9), and recrystallization from acetone produced 1.69 g (87%) white crystals of **10**. Purity: 99% (HPLC); $R_f = 0.94$ (hexanes/EtOAc 4:1); ^{1}H NMR (200 MHz, $CDCl_3$, 20 °C, TMS): $\delta = 0.88$ (t, $^3J(H,H) = 6.4$ Hz, 18H; CH_3), 1.26 (overlapped m, 108H; $(CH_2)_9$), 1.78 (m, 12H; CH_2CH_2OPh), 3.94 (m, 12H; CH_2OPh), 5.0 (d, $^3J(H,H) = 17.6$ Hz, 12H; $PhCH_2OPh$), 6.76 (d, $^3J(H,H) = 8.6$ Hz, 4H; *meta* to CH_2OPh, 4-position), 6.88 (d, $^3J(H,H) = 8.5$ Hz, 8H; *meta* to CH_2OPh, 3.5-position), 6.98 (s, 2H; *ortho* to NHCO), 7.08 (s, 2H; *ortho* to CONH), 7.24–7.35 (m, 12H; *ortho* to CH_2OPh), 7.57 ppm (s, 1H; CONH); ^{13}C NMR (90 MHz, $CDCl_3$, 20 °C, TMS): $\delta = 14.3$, 22.9, 26.3, 29.7, 32.1, 68.2, 71.3, 75.0, 100.3, 107.1, 114.4, 128.6–130.5, 134.0,135.3,141.7, 153.2, 159.2, 165.6 ppm; elemental analysis calcd (%) for $C_{127}H_{191}NO_{13}$ (M_W): C 78.62, H 9.92; found: C 78.43, H 10.20.

2-Ethoxy-7-hydroxy-benzo[1,3]dioxole-5-carboxylic acid methyl ester (11): Compound **7** (50 g, 0.27 mol), triethyl orthoformate (150 mL) and a few grains of Amberline-120 resin under N_2 were added to a 250 mL three-necked round bottomed flask containing a Teflon coated magnetic stirring bar. The reaction mixture was heated at 130 °C for 18 h, cooled to 20 °C, and then diluted with 250 mL of $CHCl_3$. The grains of Amberline-120 were removed from the reaction mixture by filtration. The organic phase was collected, washed with saturated $NaHCO_3$ solution, H_2O and brine, and dried over anhydrous Na_2SO_4. The solvent was evaporated and the white solid was precipitated in hexane from CH_2Cl_2 solution. The crude product was purified by recrystallization from $CHCl_3$/hexanes to produce 37 g (57%) of **11** as white crystals. $R_f = 0.4$ (hexanes/EtOAc 7:3); **11** decomposes before melting; ^{1}H NMR (200 MHz, $CDCl_3$, 20 °C, TMS): $\delta = 1.27$ (t, $^3J(H,H) = 7.1$ Hz, 3H; CH_3), 3.75 (q, $^3J(H,H) = 7.1$ Hz, 2H; CH_2O), 3.89 (s, 3H; CO_2Me), 5.82 (s, 1H; OH), 6.95 (s, 1H; $CH(OR)_3$, 7.18 (d, $^3J(H,H) = 1.6$ Hz, 1H; *ortho* to OH), 7.41 ppm (d, $^3J(H,H) = 1.5$ Hz, 1H; *para* to OH); ^{13}C NMR (125 MHz, $CDCl_3$ and a few drops of DMSO, 20 °C, TMS): $\delta =$ 14.8, 51.7, 52, 59.3, 101.6, 109.5, 114, 119.6, 137.2, 144.8, 167 ppm; elemental analysis calcd (%) for $C_{11}H_{12}O_6$: C 54.98, H 5.03; found: C 55.24, H 5.20.

2-Ethoxy-7-[4′-(11′-hydroxyundecyloxy)benzyloxy]benzo[1,3]dioxole-5-carboxylic acid methyl ester (13): Compound **13** was synthesized by using a similar procedure as the one used for the synthesis of **5**. The reagents used were **11** (3.06 g, 13 mmol), **12** (4.18 g, 13 mmol),and K_2CO_3 (5.18 g, 37 mmol) in DMF (45 mL). Compound **13** (4.73 g, 72%) was obtained as white crystals after recrystallization from acetone. Purity: (HPLC), 99%. m.p. 59–60 °C; $R_f = 0.33$ (hexanes/EtOAc 7:3); ^{1}H NMR (200 MHz, $CDCl_3$, 20 °C, TMS): $\delta = 1.31$ (overlapped m, 19H; $(CH_2)_8$, CH_3), 1.77 (m, 2H; CH_2CH_2OPh), 3.62–3.75 (m, 4H; CH_2OH; CH_3CH_2O), 3.89–3.99 (m, 5H; CH_2OPh, CO_2Me), 5.15 ppm(s, 2H; $PhCH_2OPh$), 6.88–6.96 (m, 3H; *meta* to CH_2OPh, $CH(OR)_3$), 7.25–7.44 ppm (overlapped m, 4H; *ortho* to CH_2OPh, *ortho* to CO_2Me); ^{13}C NMR (125 MHz, $CDCl_3$, 20 °C, TMS): $\delta = 25.9–26.2$ (m), 29.4–29.8 (m), 33, 52.2, 63.3, 68.2, 71.5, 97.8, 104.1, 111.9, 114.7, 120, 123.6, 128.5, 129.7, 148.6, 159.4, 166.8 ppm; elemental analysis calcd (%) for $C_{29}H_{40}O_8$: C 67.41, H 7.80; found: C 67.64, H 7.63.

Methyl 3,4-dihydroxy-5-[4′-(11′-hydroxy-undecyloxy)benzyloxy]benzoate (14):Compound **13** (3.15 g), silica gel (18 g), and MeOH (80 mL) were placed into a 200 mL round-bottomed flask containing a Teflon coated magnetic stir bar. The mixture was refluxed for 20 h. The progress of the reaction was followed by TLC. After the reaction was completed, the temperature of the reaction mixture was cooled to 20 °C. The silica gel was filtered and rinsed with MeOH and CH_2Cl_2. The solvent was evaporated and the solids were precipitated in H_2O from MeOH, and dried in air to obtain **14** (2.55 g, 91%) as a light yellow solid, which was used in the next step without further purification. $R_f = 0$ (hexanes/EtOAc 7:3); m.p. 105–108 °C; ^{1}H NMR (200 MHz, $CDCl_3$, 20 °C, TMS): $\delta = 1.30$ (overlapped m, 16H; $(CH_2)_8$), 1.77 (m, 2H; CH_2CH_2OPh), 3.65 (t, 2H; CH_2OH), 3.88 (s, 3H; CO_2Me), 3.97 (t, 2H; CH_2OPh), 5.04 (s, 2H; $PhCH_2OPh$), 6.92 ppm (d, 2H; *meta* to CH_2OPh), 7.25–7.36 ppm (overlapped m, 4H; *ortho* to CH_2OPh, *ortho* to CO_2Me); ^{13}C NMR (125 MHz, $CDCl_3$ and a few drops of DMSO, 20 °C, TMS): $\delta = 25.7–25.9$ (m), 29–29.4 (m), 32.7, 51.7, 62.4, 68, 71, 106.8, 111.1., 114.4, 120.7, 128.2, 129.6, 138.8, 144.7, 146.3, 159, 166.7 ppm; elemental analysis calcd (%) for $C_{26}H_{36}O_7$: C 67.79, H 7.87; found: C 68.01, H 7.95.

Methyl 3,4-bis(4′-dodecyloxybenzyloxy)-5-[4′-(11′-hydroxyundecyloxy)-benzyloxy]benzoate (15): Compound **15** was synthesized by the same general procedure as the one used for the synthesis of compound **5**. The reagents used were **14** (2.55 g, 5.5 mmol), **4** (3.51 g, 11 mmol), and K_2CO_3 (4.70 g, 34 mmol) in DMF (20 mL). Compound **15** (4.41 g, 79%) was obtained as white crystals after recrystallization from acetone twice. Purity: 99% (HPLC); m.p. 70–71 °C; $R_f = 0.12$ (hexanes/EtOAc 4:1); ^{1}H NMR (200 MHz, $CDCl_3$, 20 °C, TMS): $\delta = 0.88$ (t, $^3J(H,H) = 6.4$ Hz, 6H; CH_3), 1.27 (overlapped m, 52H; $(CH_2)_x$), 1.76 (m, 6H; CH_2CH_2OPh), 3.63 (t, $^3J(H,H) = 5.9$ Hz, 2H; CH_2OH), 3.89–4.00 (overlapped m, 9H; CH_2OPh, CO_2Me), 5.03 (d, $^3J(H,H) = 6.9$ Hz, 6H; $PhCH_2OPh$), 6.74 (d, $^3J(H,H) = 6.7$ Hz, 2H; *meta* to CH_2OPh, 4 position), 6.89 $^3J(H,H) = 6.6$ Hz, 4H; *meta* to CH_2OPh, 3,5 position), 7.23–7.35 ppm (m, 8H; *ortho* to CH_2OPh, *ortho* to CO_2Me); ^{13}C NMR (90 MHz, $CDCl_3$, 20 °C, TMS): $\delta = 14.3$, 22.9, 25.9–26.3 (m), 29.7, 32.1, 33.0, 52.4, 63.3, 68.2, 71.3, 74.9, 109.3, 114.5, 125.2, 128.7–130.5, 142.4, 152.8, 159.2, 166.9 ppm; elemental analysis calcd (%) for $C_{29}H_{40}O_8$: C 67.41, H 7.80; found: C 67.64, H 7.63.

3,4-Bis(4′-dodecyloxybenzyloxy)-5-[4′-(11′-hydroxyundecyloxy)benzyloxy] benzoic acid (16): Compound **16** was synthesized by the same general procedure as the one described for the synthesis of **9**, from compouund **15** (3.8 g) in EtOH (50 mL), 3.42 g (91%) of **16** was obtained as white crystals after recrystallization from acetone. Purity: 99% (HPLC). m.p. 85–86 °C; $R_f = 0.1$ (hexanes/EtOAc 4:1); ^{1}H NMR (200 MHz, $CDCl_3$, 20 °C, TMS): $\delta = 0.88$ (t, $^3J(H,H) = 6.1$ Hz, 6H; CH_3), 1.26 (overlapped m, 52H; $(CH_2)_x$), 1.77 (m, 6H; CH_2CH_2OPh), 3.63 (t, $^3J(H,H) = 6.5$ Hz, 2H; CH_2OH), 3.93 (m, 6H; CH_2OPh), 5.00 (d, $^3J(H,H) = 4.8$ Hz, 6H; $PhCH_2OPh$), 6.73 (d, $^3J(H,H) = 8.3$ Hz, 2H; *meta* to CH_2OPh, 4 position), 6.86 ppm (d, $^3J(H,H) = 8.3$ Hz, 4H; *meta* to CH_2OPh, 3,5 position), 7.21–7.40 ppm (overlapped m, 8H; *ortho* to CH_2OPh, *ortho* to CO_2H); ^{13}C NMR (90 MHz, $CDCl_3$, 20 °C, TMS): $\delta = 14.3$, 22.9, 25.9–26.3 (m), 29.7, 32.1, 32.9, 63.3, 68.2, 71.2, 74.9, 109.3, 114.5, 124.3, 128.6–130.5 (m), 143.3, 152.8, 159.2, 171.2 ppm

3,4-Bis(4′-dodecyloxybenzyloxy)-5-[4′-(11′-methacryloxyundecyloxy)benzyloxy]benzoic acid (18): Compound **16** (3.2 g, 3.22 mmol), dry Et_3N (1.40 mL, 10 mmol), and dry CH_2Cl_2 (20 mL) were added under N_2 to a 100 mL flask. Methacryloyl chloride (1 g, 9.6 mmol) was added drop wise at 0 °C, and the reaction was stirred at 20 °C overnight. The reaction mixture was concentrated and precipitated in MeOH. After filtration, the light yellow solids were dissolved in pyridine (30 mL) and H_2O (4 mL). The mixture was heated to 130 °C for 2 h to cleave the mixed ester anhydride **17**. After acidification with dilute HCl at 0 °C, the reaction mixture was extracted with Et_2O. The organic layer was washed with $NaHCO_3$ solution (5%) and dried over anhydrous $MgSO_4$. The solvent was evaporated, and the crude product was purified by column chromatography (SiO_2, hexanes/EtOAc 4:1) to yield **18** (2.56 g, 75%) as white crystals after recrystallization from acetone. Purity: 99% (HPLC); $R_f = 0.2$ (hexanes/EtOAc 4:1); ^{1}H NMR (200 MHz, $CDCl_3$, 20 °C, TMS): $\delta = 0.88$ (t, $^3J(H,H) = 6.4$ Hz, 6H; CH_3), 1.27 (overlapped m, 50H; $(CH_2)_x$), 1.75 (m, 8H; CH_2CH_2OPh, CH_2CH_2OCOR), 1.94 (m, 3H; $CH_3C=CH_2$), 3.94 (m, 6H; CH_2OPh), 4.14 (t, $^3J(H,H) = 6.6$ Hz, 2H; CH_2OCOR), 5.04 (d, $^3J(H,H) = 5.0$ Hz, 6H; $PhCH_2OPh$), 5.54 (m, 1H; $H_2C=CR_2$, *trans*), 6.09 (m, 1H; $H_2C=CR_2$, *cis*), 6.75 (d, $^3J(H,H) = 8.5$ Hz, 2H; *meta* to CH_2OPh, 4-position), 6.89 ppm (d, $^3J(H,H) = 8.7$ Hz, 4H; *meta* to CH_2OPh, 3,5-position), 7.23–7.42 ppm (overlapped m, 8H; *ortho* to CH_2OPh, *ortho* to CO_2H); ^{13}C NMR (90 MHz, $CDCl_3$, 20 °C, TMS): $\delta = 14.3$, 18.5, 22.9, 26.2, 29.6, 32.1, 65.1, 68.2, 71.2, 74.9, 109.9, 114.5, 124.2, 125.4, 128.6–130.5 (m), 136.7, 143.4,

152.8, 159.2, 167.8, 171.7 ppm; elemental analysis calcd (%) for $C_{67}H_{98}O_{10s}$: C 76.14, H 9.58; found: C 75.98, H 9.43.

***N*-[3,4,5-Tris(4′-dodecyloxybenzyloxy)phenyl]-3,4-bis(4′-dodecyloxybenzyloxy)-5-[4′-(11′-methacryloxyundecyloxy)benzyloxy]benzamide (19)**: Compound **19** was synthesized by the same procedure as the one described for the synthesis of compound **10**. Starting from **18** (1.25 g, 1.18 mmol), **6** (1.13 g, 1.18 mmol), DCC (485.7mg, 2.35 mmol), and DPTS (69.2 mg, 0.24 mmol) in dry THF (20 ml), **19** (1.65 g, 70%) was obtained as white crystals after purification by column chromatography (SiO_2, hexanes/EtOAc 9:1), and recrystallization from acetone. Purity: 99% (HPLC); $R_f = 0.72$ (hexanes/EtOAc 4:1); ^{1}H NMR (200 MHz, $CDCl_3$, 20 °C, TMS): $\delta = 0.88$ (t, $^3J(H,H) = 6.3$ Hz, 15H; CH_3), 1.26 (overlapped m, 104H; $(CH_2)_9$), 1.74 (m, 14H; CH_2CH_2OPh, CH_2CH_2OCOR), 1.94 (s, 3H; $CH_3C=CH_2$), 3.94 (m, 12H; CH_2OPh), 4.13 (t, $^3J(H,H) = 6.6$ Hz, 2H; CH_2OCOR), 5.02 (m, 12H; $PhCH_2OPh$), 5.54 (s, 1H; $H_2C=CR_2$, *trans*), 6.09 (s, 1H; $H_2C=CR_2$, *cis*), 6.76 (d, $^3J(H,H) = 8.1$ Hz, 4H; *meta* to CH_2OPh, 4 position), 6.88 (d, $^3J(H,H) = 8.1$ Hz, 8H; *meta* to CH_2OPh, 3,5 position), 6.99 (s, 2H; *ortho* to NHCO), 7.09 (s, 2H; *ortho* to CONH), 7.24–7.35 (overlapped m, 12H; *ortho* to CH_2OPh), 7.51 ppm (s, 1H; CONH); ^{13}C NMR (90 MHz, $CDCl_3$, 20 °C, TMS): $\delta = 14.3$, 18.5, 22.9, 26.2, 29.7, 32.0, 65.0, 68.2, 71.3, 75.0, 100.3, 107.1, 114.5, 125.4, 128.6–130.5 (m), 134.1,135.3, 136.7, 141.7, 153.2, 159.2, 165.7, 167.8 ppm; elemental analysis calcd (%) for $C_{130}H_{193}O_{15}N$: C 77.67, H 9.67; found: C 77.51, H 9.80.

Polymerization of 19: Monomer **19** was polymerized as 50% (w/v) solution in benzene under argon at 60 °C for 18 h. AIBN (1% w/w) was used as radical initiator. The polymerization solution was degassed by three freeze-pump-thaw cycles before the polymerization was initiated. Polymer **20** was then separated from unreacted monomer by column chromatography (neutral alumina, hexanes). Finally, the purified polymer **20** was dissolved in CH_2Cl_2 and precipitated in cold methanol to yield **20** (0.95 g, 79%) as a light yellow solid; $M_n = 49\,813$ and $M_w/M_n = 1.62$ (GPC with polystyrene standards).

Preparation of the binary mixtures of 10 with polymer 20: The binary mixture of **20** with **10** (**20**/**10** (*x*:*y*)) was prepared by weighing the individual components in a glass vial and then adding dry THF to give an equal final volume of a homogeneous solution. Solvent was removed under a gentle stream of dry N_2 and the mixture was dried under vacuum for 12 h at 20 °C.

Acknowledgement

Financial support by ONR and the National Science Foundation (DMR-9996288 and DMR-0102459) is gratefully acknowledged. We are also grateful to Professor S. Z. D. Cheng of the University of Akron for density measurements.

[1] *Dendrimers and other Dendritic Polymers* (Eds.: J. M. J. Fréchet, D. A. Tomalia), Wiley, **2001**.

[2] G. R. Newkome, C. N. Moorefield, F. Vögtle, *Dendrimers and Dendrons. Concepts, Synthesis and Applications*, Wiley-VCH, **2001**.

[3] For selected reviews see: a) S. M. Grayson, J. M. J. Fréchet, *Chem. Rev.* **2001**, *101*, 3819; b) D. K. Smith, F. Diederich, *Chem. Eur. J.* **1998**, *4,* 1353; c) M. Fischer, F. Vögtle, *Angew. Chem.* **1999**, *111,* 934; *Angew. Chem. Int. Ed.* **1999**, *38,* 884; d) S. Hecht, J. M. J. Fréchet, *Angew. Chem.* **2001**, *113*, 76; *Angew. Chem. Int. Ed.* **2001**, *40*, 74; e) D. Astruc, F. Chardac, *Chem. Rev.* **2001**, *101,* 2991; f) G. E. Oosterom, J. N. H. Reek, P. C. J. Kamer, P. W. N. M. van Leeuwen, *Angew. Chem.* **2001**, *113*, 1878; *Angew. Chem. Int. Ed.* **2001**, *40*, 1828; g) F. Vögtle: "*Dendrimers", Top. Curr. Chem.* **1998**, *197,* 1; h) "Dendrimers II, Architecture, Nanostructure and Supramolecular Chemistry": F. Vögtle, *Top. Curr. Chem.* **2000**, *210*, 1; i) "Dendrimers III, Design, Dimension, Function": F. Vögtle, *Top. Curr. Chem.* **2001**, *212*, 1; j) D. Seebach, P. B. Rheiner, G. Greiveldinger, T. Butz, H. Sellner, *Top. Curr. Chem.* **1998**, *197*, 125; k) J. S. Moore, *Acc. Chem. Res.* **1997**, *30,* 402.

[4] a) V. Percec, G. Johansson, J. Heck, G. Ungar, S. V. Batty, *J. Chem. Soc. Perkin Trans. 1* **1993**, 1411; b) G. Johansson, V. Percec, G. Ungar, D. Abramic, *J. Chem. Soc. Perkin Trans. 1* **1994**, 447; c) G. Ungar, S. V. Batty, V. Percec, J. Heck, G. Johansson, *Adv. Mater. Opt. Electron.* **1994**, *4*, 303; d) D. Tomazos, G. Out, J. Heck, G. Johansson, V. Percec, M. Möller, *Liq. Cryst*. **1994**, *16,* 509; e) V. Percec, G. Johansson, G. Ungar, J. Zhou, *J. Am. Chem. Soc.* **1996**, *118*, 9855; f) V. S. K. Balagurusamy, G. Ungar, V. Percec, G. Johansson, *J. Am. Chem. Soc.* **1997**, *119*, 1539; g) S. D. Hudson, H. T. Jung, V. Percec, W. D. Cho, G. Johansson, G. Ungar, V. S. K. Balagurusamy, *Science* **1997**, *278*, 449; h) V. Percec, W. D. Cho, P. E. Mosier, G. Ungar, D. J. P. Yeardley, *J. Am. Chem. Soc.* **1998**, *120*, 11 061; i) V. Percec, C. H. Ahn, T. K. Bera, G. Ungar, D. J. P. Yeardley, *Chem. Eur. J.* **1999**, *5*, 1070; j) G. Ungar, V. Percec, M. N. Holerca, G. Johansson, J. Heck, *Chem. Eur. J.* **2000**, *6*, 1258; k) V. Percec, W. D. Cho, M. Möller, S. A. Prokhorova, G. Ungar, D. J. P. Yeardley, *J. Am. Chem. Soc.* **2000**, *122*, 4249; l) V. Percec, W. D. Cho, G. Ungar, D. J. P. Yeardley, *Angew. Chem.* **2000**, *112*, 1661; *Angew. Chem. Int. Ed.* **2000**, *39*, 1597; m) V. Percec, W. D. Cho, G. Ungar, *J. Am. Chem. Soc.* **2000**, *122*, 10 273; n) V. Percec, W. D. Cho, G. Ungar, D. J. P. Yeardley, *J. Am. Chem. Soc.* **2001**, *123*, 1302; o) W. J. Pao, M. R. Stetzer, P. A. Heiney, W. D. Cho, V. Percec, *J. Phys. Chem. B.* **2001**, *105,* 2170; p) V. Percec, M. N. Holerca, S. Uchida, W. D. Cho, G. Ungar, Y. Lee, D. J. P. Yeardley, *Chem. Eur. J.* **2002**, *8*, 1106; q) V. Percec, W. D. Cho, G. Ungar, D. J. P. Yeardley, *Chem. Eur. J.* **2002**, *8*, 2011; r) J. A. A. W. Elemans, M. J. Boerakker, S. J. Holder, A. E. Rowan, W. D. Cho, V. Percec, R. J. M. Nolte, *Proc. Natl. Acad. Sci. USA* **2002**, *99*, 5093; s) V. Percec, M. Glodde, T. K. Bera, Y. Miura, I. Shiyanovskaya, K. D. Singer, V. S. K. Balagurusamy, P. A. Heiney, I. Schnell, A. Rapp, H. W. Spiess, S. D. Hudson, H. Duan, *Nature* **2002**, *419*, 384.

[5] a) V. Percec, C. H. Ahn, G. Ungar, D. J. P. Yeardley, M. Möller, S. S. Sheiko, *Nature* **1998**, *391*, 161; b) V. Percec, C. H. Ahn, W. D. Cho, A. M. Jamieson, J. Kim, T. Leman, M. Schmidt, M. Gerle, M. Möller, S. A. Prokhorova, S. S. Sheiko, S. Z. D. Cheng, A. Zhang, G. Ungar, D. J. P. Yeardley, *J. Am. Chem. Soc*. **1998**, *120*, 8619; c) V. Percec, D. Schlueter, G. Ungar, S. Z. D. Cheng, A. Zhang, *Macromolecules* **1998**, *31*, 1745; d) V. Percec, M. N. Holerca, *Biomacromolecules* **2000**, *1,* 6; e) V. Percec, J. A. Heck, D. Tomazos, G. Ungar, *J. Chem. Soc. Perkin Trans. 2* **1993**, 2381; f) V. Percec, D. Tomazos, J. Heck, H. Blackwell, G. Ungar, *J. Chem. Soc. Perkin Trans. 2* **1994**, 31; g) V. Percec, D. Schlueter, Y. K. Kwon, J. Blackwell, M. Möller, P. J. Slangen, *Macromolecules* **1995**, *28*, 8807; h) G. Johansson, V. Percec, G. Ungar, J. P. Zhou, *Macromolecules* **1996**, *29*, 646; i) S. A. Prokhorova, S. S. Sheiko, A. Mourran, R. Azumi, U. Beginn, G. Zipp, C. H. Ahn, M. N. Holerca, V. Percec, M. Möller, *Langmuir* **2000**, *16,* 6862; j) D. J. P. Yeardley, G. Ungar, V. Percec, M. N. Holerca, G. Johansson, *J. Am. Chem. Soc.* **2000**, *122*, 1684; k) H. Duan, S. D. Hudson, G. Ungar, M. N. Holerca, V. Percec, *Chem. Eur. J.* **2001**, *7*, 4134; l) V. Percec, M. N. Holerca, S. Uchida, S. N. Magonov, D. J. P. Yeardley, G. Ungar, H. Duan, S. D. Hudson, *Biomacromolecules* **2001**, *2,* 706; m) V. Percec, M. N. Holerca, S. Uchida, D. J. P. Yeardley, G. Ungar, *Biomacromolecules* **2001**, *2,* 729; n) V. Percec, T. K. Bera, *Biomacromolecules* **2002**, *3*, 167; o) V. Percec, T. K. Bera, *Tetrahedron* **2002**, *58*, 4031; p) V. Percec, G. Zipp, G. Johansson, U. Beginn, M. Möller, *Macromol. Chem. Phys.* **1997**, *198,* 265; q) U. Beginn, G. Zipp, M. Möller, G. Johansson, V. Percec, *Macromol. Chem. Phys.* **1997**, *198,* 2839.

[6] a) V. Percec, P. Chu, G. Ungar, J. Zhou, *J. Am. Chem. Soc*. **1995**, *117,* 11 441; b) V. Percec, M. Kawasumi, *Macromolecules* **1992**, *25,* 3843; c) V. Percec, P. Chu, M. Kawasumi, *Macromolecules* **1994**, *27,* 4441.

[7] For selected examples of dendrimers that self-organize into liquid crystalline phases from other laboratories see: a) D. J Pesak, J. S. Moore, *Angew. Chem. Int. Ed. Engl*. **1997**, *36*, 1636; *Angew. Chem.* **1997**, *109*, 1709; b) H. Meier, M. Lehmann, *Angew. Chem.* **1998**, *110*, 666; *Angew. Chem. Int. Ed.* **1998**, *37,* 643; c) J. Barberá, M. Marcos, J. L. Serrano, *Chem. Eur. J.* **1999**, *5*, 1834; d) M. Marcos, R. Giménez, J. L. Serrano, B. Donnio, B. Heinrich, D. Guillon, *Chem. Eur. J.* **2001**, *7,* 1006; e) M. Suárez, J. M. Lehn, S. C. Zimmerman, A. Skoulios, B. Heinrich, *J. Am. Chem. Soc.* **1998**, *120*, 9526; f) R. Deschenaux, E. Serrano, A. H. Levelut, *Chem. Commun.* **1997**, 1577; g) M. W. P. L. Baars, S. H. M. Söntjens, H. M. Fischer, H. W. I. Peerlings, E. W. Meijer, *Chem. Eur. J.* **1998**, *4,* 2456; h) I. M. Saez, J. W. Goodby, R. M. Richardson, *Chem. Eur. J.* **2001**, *7,* 2758; i) M. Kimura, Y. Saito, K.

  0947-6539/03/0904-0934 $ 20.00+.50/0

Ohta, K. Hanabusa, H. Shirai, N. Kobayashi, *J. Am. Chem. Soc.* **2002**, *124*, 5274; j) D. Tsiourvas, K. Stathopoulou, Z. Sideratou, C. M. Paleos, *Macromolecules* **2002**, *35*, 1746; k) P. Busson, J. Örtegren, H. Ihre, U. W. Gedde, A. Hult, G. Andersson, A. Eriksson, M. Lindgren, *Macromolecules* **2002**, *35*, 1663.
[8] R. Tapia, G. Torres; J. A. Valderrama, *Synth. Commun.* **1986**, *16*, 681.
[9] B. Errazuriz, R. Tapia, J. A. Valderrama, *Tetrahedron*, **1985**, *26*, 819.
[10] B. Xu, T. M. Swager, *J. Am. Chem. Soc.* **1993**, *115*, 1159.
[11] V. Percec, D. Schlueter, J. C. Ronda, G. Johansson, G. Ungar, J. P. Zhou, *Macromolecules* **1996**, *29*, 1464.
[12] B. H. Han, D. H. Shin, S. Y. Cho, *Tetrahedron Lett.* **1985**, *26*, 6233.
[13] A. Merz, M. Rauschel, *Synthesis* **1993**, 797.
[14] a) A. M. Levelut, *J. Phys. Lett. France* **1979**, *40*, 287; b) S. Chandrasekhar, *Liquid Crystals*, 2nd ed. Cambridge University Press, **1992**; c) P. Davidson, M. Clerc, S. S. Ghosh, N. C. Maliszewskyj, P. A. Heiney, J. Hynes Jr., A. B. Smith III, *J. Phys. France II*, **1995**, *5*, 249.
[15] G. Ungar, D. Abramic, V. Percec, J. A. Heck, *Liq. Cryst.* **1996**, *21*, 73.
[16] V. Percec, C. H. Ahn, B. Barboiu, *J. Am. Chem. Soc.* **1997**, *119*, 12978.
[17] P. G. Schiemenz, H. Engelhard, *Chem. Ber.* **1959**, *92*, 862.
[18] D. Grablin, F. Merger, F. Schulte, O. Volkert, *Chem. Ber.* **1967**, *100*, 3077

Received: July 26, 2002
Revised: October 21, 2002 [F4285]

  0947-6539/03/0904-0935 $ 20.00+.50/0